Deanship of Graduate Studies

Al-Quds University

Synthesis, Characterization, and *In Vitro* Conversion Kinetics of Novel Atorvastatin Prodrugs

Buthaina Amjad Al-Jubeh

M.Sc. Thesis

Jerusalem-Palestine

1444/2022

Synthesis, Characterization and *In Vitro* Conversion Kinetics of Novel Atorvastatin Prodrugs

Prepared by:

Buthaina Amjad Al-Jubeh

B.Sc., Pharmacy, Hebron University, Palestine.

Supervised by:

Prof. Dr. Rafik Karaman

A thesis submitted in partial fulfillment of requirements for the degree of Master of Pharmaceutical Science, Al-Quds University.

1444/2022

Al-Quds University

Deanship of Graduate Studies

Pharmaceutical Sciences Program

Thesis Approval

Synthesis, Characterization, and *In Vitro* Conversion Kinetics of Novel Atorvastatin Prodrugs

Prepared by: Buthaina Amjad Al-Jubeh

Registration No.: 21712368

Supervisor: Prof. Rafik Karaman

Master thesis Submitted and Accepted, Date: December 20, 2022

The names and signatures of the examining committee members are as follows:

Head of Committee: Prof. Rafik Karaman

Signature:

Internal Examiner: Dr. Salih Al-Jabour

Signature:

External Examiner: Dr. Hatim A Hejaz

Signature:

Jerusalem–Palestine

1444/2022

Dedicated to my mother, Atika Al-Jubeh

Declaration

I certify that the thesis submitted for the degree of master is the result of my own research, except where otherwise acknowledged, and that this thesis (or any part of the same) has not be submitted for a higher degree to any other university or institution.

Signed: 

Buthaina Amjad Al-Jubeh

Date: December 20, 2022

Abstract

Hypercholesterolemia is a risk factor for the development of atherosclerotic disease. Atorvastatin is a mainstay in the prevention and treatment of hypercholesterolemia and atherosclerotic cardiovascular disease. Atorvastatin efficiently lowers increased plasma cholesterol by inhibiting 3-hydroxy-3-methylglutaryl-coenzyme A (HMG-CoA) reductase. Due to significant presystemic metabolism, atorvastatin has low oral bioavailability (14 %). By transiently modifying the structure of a substance *via* prodrug synthesis, low bioavailability, and other pharmacokinetic and/or physicochemical disadvantages, can be resolved. The synthesis of novel atorvastatin prodrugs as possible candidates for atorvastatin delivery with improved bioavailability and fewer side effects is described in this thesis. Based on Bruice's enzyme model of intramolecular reactions, three atorvastatin prodrugs were synthesized in high yield by conjugating dicarboxylic anhydride linkers (maleic anhydride, succinic anhydride, and phthalic anhydride) to the hydroxyl groups of atorvastatin; in order to create prodrug systems with intramolecular hydrolysis ability. The prodrugs are expected to have greater bioavailability, because they hide the metabolically labile functional groups, and increased water solubility. Melting point, FT-IR, LC-MS, and ^{1}H-NMR analyses were used to confirm the identity of the produced prodrugs. The intramolecular hydrolysis of the three prodrugs in different media was studied *in vitro* and found to have varying conversion rates or no conversion. The prodrug containing the maleate linker (proD1) was completely hydrolyzed in 0.1N acid solution, pH 3 buffer, and human plasma, at half-lives of 102 hours, 161 hours, and 198 hours, respectively. The succinate-linked prodrug (proD2) was degraded in acidic medium exclusively (pH 3) and had a half-life of 216 hours. The pH of the medium influenced prodrug intraconversion, which was quicker in acidic conditions. Furthermore, prodrug intraconversion was dependent on the structural characteristics of the connected prodrug linker,

and the intramolecular reaction was achieved in a strained prodrug system with a favorable proximity orientation.

Table of Contents

List of Schemes and Figures

List of Abbreviations

ADEPT	Antibody-directed enzyme prodrug therapy
ADME	Absorption, distribution, metabolism and elimination
apo B-100	Apoprotein B-100
CES1	Carboxylesterase 1
CETP	Cholesterol ester transfer protein
CVD	Cardiovascular disease
CYP	Cytochrome P450
d	Doublet
dd	Doublet of doublets
DEPT	Directed enzyme prodrug therapy
DFT	Density functional theory
D_2O	Deuterated water
eq	Equivalent
FDA	Food and Drug Administration
FH	Familial hypercholesterolemia
FT-IR	Fourier transform infrared
GDEPT	Gene-directed enzyme prodrug therapy
HCl	Hydrochloric acid
HDL	High density lipoproteins
HLB	Hydrophilic lipophylic balance
HMG-CoA	3-hydroxy- 3-methylglutaryl-coenzyme A
^{1}H-NMR	Proton nuclear magnetic resonance
IDL	Intermediate density lipoproteins
LDL	Low density lipoproteins
LPL	Lipoprotein lipase
m	Multiplet
M/z	Mass to charge ratio
MI	Myocardial infarction
MM	Molecular mechanics

mM	millimolar
N	Normal
NaH	Sodium hydride
NaOH	Sodium hydroxide
NS	Solid nano-suspension
o/w	Oil in water
OATP	Organic anion-transporting polypeptide
PCSK9	Proprotein convertase subtilisin/kexin type 9
pH	Potential of hydrogen
PPARα	Peroxisome proliferator-activated receptor α
ppm	Part per million
ProD	Prodrug
QM	Quantum mechanical
R^2	Determination coefficient
RP	Reverse phase
s	Singlet
SN_2	Substitution nucleophilic bimolecular
SNEDDS	Self-nanoemulsifying drug delivery system
t	Triplet
t½	Half life
UPLC	Ultra-performance liquid chromatography
v/v	Volume per volume
VDEPT	Virus-directed enzyme prodrug therapy
VLDL	Very low density lipoproteins

Chapter One

Introduction

1. Chapter 1: Introduction

1.1. Background

1.1.1. Plasma lipoproteins

Cholesterol is an essential structural component of plasma membranes, it can be obtained from dietary sources, or is synthesized endogenously in hepatocytes [1]. Cholesterol is transported throughout the body within particles called plasma lipoproteins. Plasma lipoproteins are macromolecular complexes composed of a lipid core and a surface coat of proteins [2, 3]. The major function of plasma lipoproteins is to transport free fatty acids and cholesterol in the plasma for cellular metabolism; to be used for energy use, steroid hormone and vitamin D production, lipid deposition, and bile acid formation [4, 5]. There are four major classes of plasma lipoproteins, which are divided according to their hydrated density that determines their flotation characteristics during ultracentrifugation [6]. The main classes are: chylomicrons, very low density lipoproteins (VLDL), low density lipoproteins (LDL), and high density lipoproteins (HDL). Intermediate density lipoproteins (IDL) have been isolated and identified as well. The most abundant lipid constituents of plasma lipoproteins are triglycerides, phospholipids, unesterified cholesterol, and cholesterol esters [3, 7]. The protein constituents of plasma lipoproteins are called apolipoproteins or apoproteins. Apoproteins are required to solubilize the hydrophobic lipids in the circulation and to recognize specific cell membrane receptors, which direct the associated lipoproteins' metabolism, and they act as well as cofactors for enzymes involved in the metabolism of lipoproteins [6, 8]. Lipoproteins vary in the amount of apoproteins, triglycerides, esterified and unesterified cholesterol, and phospholipids contained in each type of particle [9].

Chylomicrons are the primary lipoproteins associated with the absorption of dietary fats and cholesterol. In intestinal cells, dietary cholesterol is initially packed with large amounts of

triglycerides into chylomicron micelles with seven carrier apoproteins. Chylomicrons are broken down by lipoprotein lipase (LPL), which hydrolyzes the triglyceride core, and the fatty acids are used for energy or stored in adipose tissue; while the chylomicron remnants are cleared by the liver [5, 9]. In the liver, VLDLs, the major carrier of endogenous triglycerides, are produced and secreted into the bloodstream. VLDLs are metabolized by LPL, releasing free fatty acids and IDLs which are then converted into LDLs. LDLs carry a core of cholesterol esters and small amounts of triglycerides. LDLs are the major cholesterol transporters around the body, and the main atherogenic lipoproteins [10].

LDL particles are associated with apoprotein (apo) B-100, which is the ligand for the LDL receptor in the liver [6]. LDLs are taken up by the liver and (to a lesser extent) peripheral tissues for useful biologic functions. The internalization and degradation of LDL particles in the liver depend on the binding of LDL particles to hepatocytes' surface receptors (LDL-receptors). The LDL receptor protein is synthesized in the hepatocytes' endoplasmic reticulum, and is matured within the Golgi apparatus, then the receptors are expressed on the cell surface. Binding of LDL receptors to LDL particles, specifically to ApoB-100 of the particle, leads to the uptake of the complex by endocytosis. The LDL particle then undergoes lysosomal degradation and the receptor molecule is recycled [7, 11]. LDL uptake at the liver leads to bile acid formation, which plays a role in the digestion of cholesterol and fat. Non-hepatic LDL-cholesterol is used for cell membrane synthesis and steroid production [9].

In contrast to LDLs, HDLs are antiatherogenic lipoproteins. HDLs consist of small, lipid poor particles produced in the liver and intestinal cells. The nascent HDL particles are converted to HDLs by incorporating cholesteryl esters liberated from peripheral tissues, which are then

transferred to the liver by cholesterol ester transfer protein (CETP). Thereby, HDLs are involved in reverse cholesterol transport from peripheral tissues to the liver, removing excess cholesterol from cells, hence the HDL's antiatherogenic effects [7-9].

1.1.2. Hyperlipidemia

LDLs and HDLs regulate the amount of cholesterol in the body, an imbalance of these lipoproteins can increase the risk of cardiovascular events. Elevated levels of blood lipids are related to morbidity condition called hyperlipidemia. Hyperlipidemia refers to a variety of diseases related to increased levels of cholesterol or triglycerides or both, resulting from increased production or delayed degradation of atherogenic lipoproteins, or decreased production or increased degradation of protective lipoproteins [9].

There is a well-established association between hyperlipidemia and the risk of cardiovascular disease (CVD) including myocardial infarction (MI) and stroke. Cardiovascular morbidity and mortality risk is reduced by therapeutic management to lower cholesterol levels. [12, 13]. Elevated LDL-cholesterol can lead to atherosclerotic cardiovascular disease; subendothelial retention of LDL-cholesterol has been proposed to initiate atherosclerosis and its clinical sequelae of coronary artery disease, peripheral vascular disease, stroke, aneurysm formation, and sudden death [13-15]. On the other hand, increased levels of HDL-cholesterol (≥60 mg/dL) can decrease the risk [16].

Hyperlipidemia arises from hereditary factors (primary) or acquired conditions (secondary). Familial forms of hyperlipidemia represent less than 20% of all dyslipidemias [9], most lipid disorders are polygenic metabolic derangement induced by diets high in saturated or trans fats, obesity, sedentary lifestyles, some diseases such as hypothyroidism, biliary obstruction, type 2

diabetes mellitus, hypertension, renal disease, hepatoma, alcoholism, and some drugs like cyclosporine, glucocorticoids, and thiazide diuretics [12, 17].

The presence of high plasma cholesterol levels, as a consequence of the rise of LDLs, with normal plasma triglycerides is defined as hypercholesterolemia [18]. Familial hypercholesterolemia (FH) is a relatively common (1 in 500 individuals) autosomal dominant disorder [19]. Total cholesterol usually exceeds 300 mg/dL for heterozygotes. Homozygotes are rare but have total cholesterol above 600 mg/dL, and patients usually die of MI early, prior age of 20 years, if not treated [13]. FH is characterized clinically by tendon xanthomas, arcus cornea, and premature coronary artery disease [13, 18]. FH includes different phenotypes of different mutations of the LDL receptor gene in which synthesis of the receptor is defective, intracellular transport of LDL receptor protein from the endoplasmic reticulum to the Golgi apparatus is blocked, the LDL receptor binding protein is defective, or the internalization of the receptor-LDL complex is defective. Familial defective apoB-100 is a FH-clinically-identical autosomal dominant disorder in which the defect is in the ApoB-100 ligand on the LDL particle, rather than the receptor itself [9, 20].

Hyperlipidemia includes other forms such as hypertriglyceridemia, characterized by serum triglycerides greater than 200 mg/dL, and mixed hyperlipidemia, in which both cholesterol and triglyceride levels are elevated [9, 18].

1.1.3. Hyperlipidemia drug therapy

1.1.3.1. Statins

Statins reduce total cholesterol and LDL-cholesterol *via* the inhibition of 3-hydroxy- 3-methylglutaryl-coenzyme A (HMG-CoA) reductase, which is the enzyme involved in the rate

limiting step of cholesterol biosynthesis. As a result, hepatic uptake of LDL is increased leading to increased removal of LDL from the plasma [21].

Statins are the mainstay of treatment of hyperlipidemia. Large-scale clinical trials have clearly shown that statins effectively lower LDL-cholesterol levels, reduce the risk of developing CVD in patients with elevated LDL-cholesterol, and reduce mortality and disease progression among patients with clinical atherosclerotic-CVD [17, 22-25].

Currently, the United States Food and Drug Administration (FDA) has approved seven drugs of the statin class (atorvastatin, fluvastatin, lovastatin, pitavastatin, pravastatin, rosuvastatin, and simvastatin) for the treatment of hyperlipidemia in combination with a heart-healthy diet [26-32]. Statins vary in the degree of LDL-cholesterol lowering for a given dose, they can reduce LDL-cholesterol by approximately 20% to 65%; the greater reductions are seen with atorvastatin and rosuvastatin. Pitavastatin, lovastatin, and simvastatin have moderate reductions, and the lowest reductions are seen with fluvastatin and pravastatin [33-35]. All statins except pivastatin are indicated for familial hypercholesterolemia [36]. Patients receiving statins commonly experience muscle-related adverse events, which may contribute to poor adherence and no persistence of treatment [37].

1.1.3.2. Non-statins

Statins are the preferred medical treatment to lower elevated LDL-cholesterol for most patients [17]. However, several other-classes drugs are available to augment for patients who do not respond adequately to statins, or substitute for patients who are intolerant to statins, or when statins are contraindicated. These drugs include bile acid sequestrants, ezetimibe, fibrates, niacin, and the

recently approved proprotein convertase subtilisin/kexin type 9 (PCSK9) inhibitors, lomitapide, and mipomersen [36, 38].

Bile acid sequestrants, like cholestyramine, colestipol, and colesevelam, reduce cholesterol levels by binding bile acids within the intestines and impeding biliary cholesterol reabsorption and enterohepatic cycling, increasing hepatic LDL receptors and leading to cholesterol clearance by conversion to bile acids [39]. Bile acid sequestrants are synergistic in their LDL lowering with other lipid-lowering drugs [40].

Ezetimibe reduces LDL levels by inhibiting dietary and biliary cholesterol absorption in the intestines, by blocking the Niemann-Pick C1 receptor [41]. Ezetimibe has a synergistic effect with statins and is suggested to be the first drug to be used in combination therapy with statins when combination therapy is needed [42, 43].

Fibrates or fibric acid derivatives, such as gemfibrozil and fenofibrate, are agonists of peroxisome proliferator-activated receptor α (PPARα), they are associated with significant triglyceride lowering, LDL-cholesterol lowering and HDL-cholesterol increase. Fibrates have been shown to reduce major coronary events [44, 45]. Although combination with statins further reduce LDL-cholesterol, fibrates can increase the risk of statin related myopathy and rhabdomyolysis [46].

Niacin inhibits the hepatic production of VLDL and therefore reduces LDL-cholesterol, it also increases levels of HDL by delaying clearance and reducing the transfer of cholesterol from HDL to VLDL [47]. Results from multiple studies indicated that the addition of niacin to statins increase the risk of statin adverse events, and failed to show that combination reduces the risk of cardiovascular events [48].

Recently, a new class of medications for lowering LDL-cholesterol called proprotein convertase subtilisin/kexin type 9 (PCSK9) inhibitors has been approved. Alirocumab and evolocumab are monoclonal antibodies that are administered by subcutaneous injection and bind to PCSK9. Normally, PCSK9 increase the degradation of LDL receptors, when PCSK9 is inhibited, more LDL receptors remain in circulation, which then lower LDL-cholesterol [49].

Another two lipid-lowering drugs have recently been approved for homozygous familial hypercholesterolemia; to be used in combination with other lipid lowering therapy, lomitapide, and mipomersen. Lomitapide is an oral microsomal triglyceride transfer protein inhibitor. Lomitapide reduces the secretion of chylomicron and VLDL into the circulation, lowering plasma LDL-cholesterol levels [50]. Mipomersen, administered by subcutaneous injection, is an antisense oligonucleotide that inhibits apoB-100 synthesis, leading to reduced secretion of VLDL and lowering plasma LDL-cholesterol levels [51].

1.2. Atorvastatin

Atorvastatin ([R-(R*, R*)]-2-(4-fluorophenyl)-ß, δ-dihydroxy-5-(1-methylethyl)-3-phenyl-4-[(phenylamino)carbonyl]-1H-pyrrole-1-heptanoic acid, **Figure 1.1.a**) is a synthetic lipid lowering drug of the statin class, introduced by Pfizer as Lipitor® [26]. Atorvastatin is a competitive inhibitor of 3-hydroxy-3-methylglutaryl-coenzyme A (HMG-CoA) reductase, HMG-CoA reductase is the enzyme responsible for the conversion of HMG-CoA to mevalonate, which is the rate limiting step in the synthesis of cholesterol in the liver [52] **(Figure 1.2)**. By blocking the conversion of HMG-CoA to mevalonate, atorvastatin decreases the production of cholesterol in the liver, and leads to an increase in the expression of LDL receptors on hepatic cells' surfaces through a negative feedback loop, LDL receptors then remove LDL-cholesterol from plasma.

Consequently, atorvastatin reduces the levels of total and low density lipoproteins as well as triglycerides, and it also increases the level of HDL [53, 54].

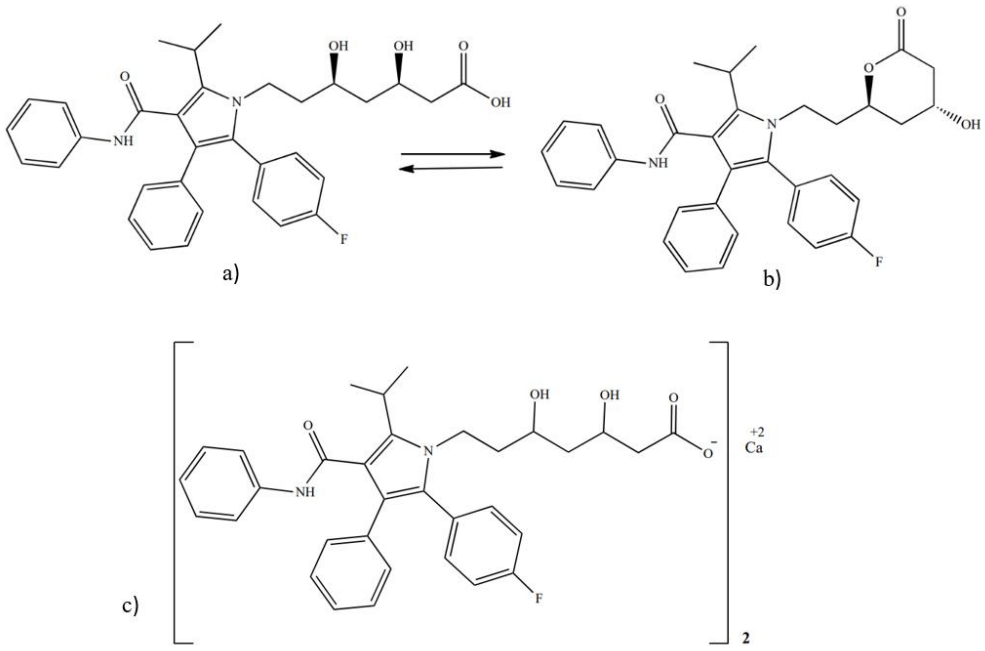

Figure 1. 1: Chemical structures of atorvastatin acid (a), atorvastatin lactone (b), and atorvastatin calcium (c).

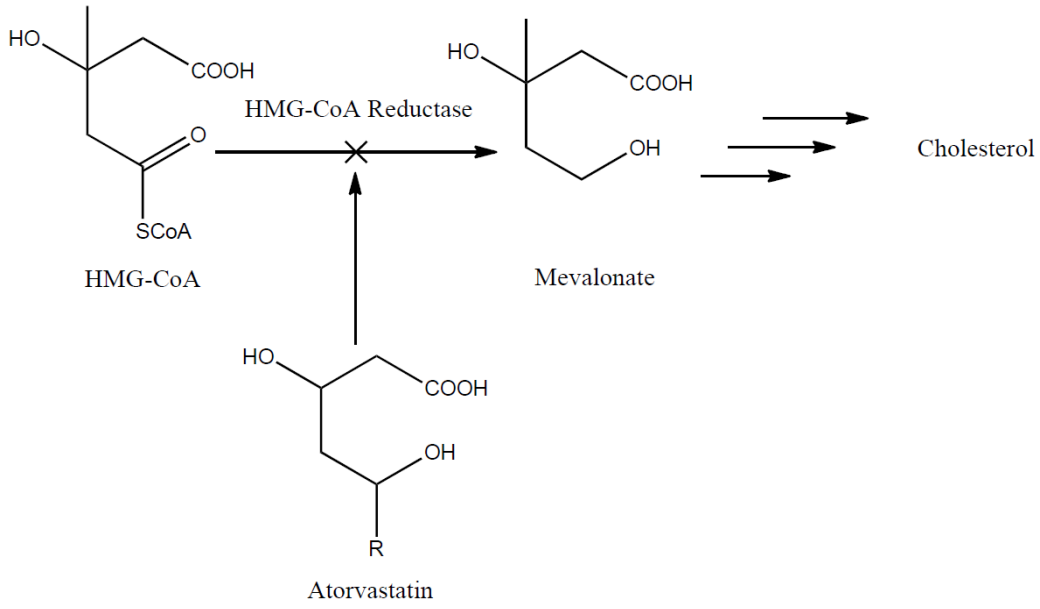

Figure 1. 2: Mechanism of action of atorvastatin: Inhibition of HMG-CoA reductase in hepatocytes, and thus blocking the conversion of HMG-CoA to mevalonate, a precursor of cholesterol.

Atorvastatin, as atorvastatin calcium, is available in tablets in strengths of 10-80 mg [26]. Atorvastatin is used in the management of hypercholesterolemia, the drug induces regression of atherosclerosis and lowers the risk of cardiovascular events [54]. Statins in general are considered the treatment of choice for hypercholesterolemia, clinical studies have demonstrated atorvastatin to be the second most effective statin for reducing LDL-cholesterol [21]. Atorvastatin in dosages of 10, 20, 40, and 80 mg/day achieved reductions in serum LDL-cholesterol levels of 39%-60% in various trials. The reductions were significantly higher than that of pravastatin, simvastatin, and fluvastatin, and slightly lower than that of rosuvastatin [55]. In large scale, long-term trials in patients with primary hypercholesterolemia, atorvastatin produced the highest reductions in levels of total cholesterol, LDL-cholesterol, and triglyceride compared to other statins [56].

Atorvastatin is indicated for the prevention of cardiovascular disease in patients with a risk of coronary heart disease. In patients with coronary heart disease, atorvastatin is used to reduce the risk of myocardial infarction, stroke, revascularization procedures, and angina. The drug is indicated as an adjunct to diet to reduce elevated total-cholesterol, LDL, apoB, and triglyceride levels, and to increase HDL levels in adult patients with primary hypercholesterolemia and mixed dyslipidemia; and to reduce total cholesterol, LDL-cholesterol, and apoB levels in patients 10 to 17 years of age, with some cases of heterozygous familial hypercholesterolemia. Atorvastatin is also used for the treatment of patients with primary dysbetaliproteinemia (high levels of cholesterol and triglycerides), who do not respond adequately to diet, and for the treatment of patients with elevated serum triglycerides levels. Atorvastatin is also used as an adjunct to other lipid lowering treatments to reduce total cholesterol and LDL-cholesterol in patients with homozygous familial hypercholesterolemia [57-59].

1.2.1. Pharmacokinetics of atorvastatin

Atorvastatin is present either in the acid form **(Figure 1.1.a)** or the lactone form **(Figure 1.1.b)**, the free hydroxyl acid form of atorvastatin is unstable and it converts easily to the lactone form, which is 15 times less soluble in water than the acid form [60, 61]. Therefore, atorvastatin in pharmaceutical formulations is combined with alkaline earth-metal salt (calcium) as atorvastatin calcium **(Figure 1.1.c)**. Atorvastatin calcium is slightly soluble in water. Atorvastatin is highly permeable through intestinal membranes, thus the drug is rapidly and completely absorbed after oral administration with a maximum plasma concentration at 1 to 2 hours [26, 62]. However, the absolute oral bioavailability of atorvastatin is only 14%, this is attributed to extensive presystemic clearance in gastrointestinal mucosa and first pass metabolism in the liver. The rate and extent of

atorvastatin absorption are decreased by food. The mean volume of distribution of atorvastatin acid is 381liters, and plasma protein binding exceeds 98% [26].

Atorvastatin is subject to clearance in both the gut and the liver by cytochrome P450-3A4 (CYP 3A4) and cellular membrane transport. Atorvastatin acid is extensively metabolized by oxidation, lactonisation, and glucuronidation; the metabolites are eliminated by secretion in bile and direct secretion from blood to the gastrointestinal tract. Atorvastatin is a substrate for P-glycoprotein, organic anion-transporting polypeptide (OATP) C, and H^+-monocarboxylic acid cotransporters *in vitro*. *In vivo*, atorvastatin is metabolized by CYP 3A4 to ortho- and para-hydroxylated active metabolites, and to various beta oxidation inactive metabolites. Atorvastatin and its metabolites are mainly eliminated in bile; the renal route is of minor importance (<1%). The half-life of atorvastatin is 14 hours and the half-life of its active metabolites is 20-30 hours [26, 56].

1.2.2. Atorvastatin adverse effects

Statins are proven to be the main therapy for the prevention and treatment of cardiovascular disease. Nevertheless, treatment with atorvastatin, and other statins, is associated with adverse effects that are dose dependent [63, 64]. Evidence suggests that as many as 20% of patients with a clinical indication for statin treatment are unable to take a daily statin due to some degree of intolerance [65], and 40–75% of patients discontinue their statin therapy within one year after initiation [66].Common adverse effects in patients taking atorvastatin include nasopharyngitis, dyspepsia, diarrhea, arthralgia, fatigue, and pain in the extremities [26]. Myopathies have been noted in patients taking atorvastatin, these myopathies include muscle aches, muscle tenderness, or muscle weakness with elevated creatine phosphokinase > 10x the upper limit of normal [67]. The spectrum of statin-related myopathies ranges from common mild myalgia to rare, but fatal,

rhabdomyolysis (extensive muscle damage that results in the release of cellular contents into the systemic circulation) [68-70]. The risk of atorvastatin-induced myopathies and rhabdomyolysis is increased significantly when drug interactions occur with other medications such as azole antifungals, fibrates, cyclosporine, macrolide antibacterial, and HIV protease inhibitors [71, 72]. Other predisposing risk factors for statin-related myopathy include the presence of renal or hepatic disease, advancing age, and being female [63, 73].Management of statin-induced myopathies includes temporarily holding therapy, switching to an alternative, or reducing the dose [69, 74].

1.3. Prodrugs

The conventional discovery and development of new drugs is a laborious, costly, and lengthy process that requires an average of 10-15 years [75, 76]. Unfortunately, some drug candidates fail to attain the desired clinical profile in order to be used *in vivo*. As a result, a large portion of new drug candidates fails in the development process. Poor pharmacokinetics and toxicity are the main causes of high attrition rates in drug development. Therefore, resolving the pharmacokinetic and toxicological properties of drug candidates is of high importance to improve the efficiency and cost-effectiveness of the drug industry. The prodrug approach is a relatively fast and easy way to develop drugs by improving unfavorable physicochemical, biopharmaceutical, and/or pharmacokinetic properties of already existing drugs and drug candidates [76]. Even more, prodrugs have evolved from being used as a salvage strategy to being intentionally designed [77]. Over the past two decades, the market share of prodrugs has grown noticeably. Approximately 10% of all marketed medicines are prodrugs, and prodrugs compromised 20% of all small molecule drug approvals over the past several years [78, 79].

A prodrug is an inactive (or poorly active) chemically modified version of a pharmacologically active agent, which must undergo transformation *in vivo* to release the active drug [80, 81]. The term prodrug was first introduced by Adrian Albert in 1958 [82]. The basic aim of prodrug design is to optimize the absorption, distribution, metabolism, and elimination (ADME) properties of drugs and drug candidates by masking undesirable drug properties such as: low solubility in water or in lipid membranes, chemical instability, undesirable taste, irritation, or pain after local administration, low target selectivity, presystemic metabolism, and toxicity [78, 80, 81].

Prodrugs are classified into two major classes; carrier-linked prodrugs and bioprecursors. Carrier-linked prodrugs are the common prodrugs, the active molecule is temporarily linked to a carrier (linker) through a bio-reversible covalent linkage. Carriers are commonly attached by chemical groups such as ester, amide, carbonate, carbamate, ether, phosphate, imine, among others; and the carrier is removed by a chemical or enzymatic reaction. It is important that after the achievement of the prodrug goal, it must degrade to the active drug and a nontoxic moiety, and the released linker should be eliminated rapidly [80, 83].

In carrier linked prodrugs, when the carrier is linked directly to the parent drug, the prodrug is sub-classified as bipartite. When a spacer is used to link the carrier to the parent drug, the prodrug is sub-classified as tripartite. A special type of carrier linked prodrugs is the mutual prodrugs (co-drugs), in which two active compounds are linked to each other, each acting as the carrier to the other, to increase effectiveness through synergistic action [76].

Unlike carrier linked prodrugs, bioprecursor prodrugs do not have carriers, but result from a molecular modification of the active compound itself, they are converted to an active drug after metabolic reactions, such as oxidation or reduction [84, 85].

1.3.1. Applications of the prodrug approach

Basically, prodrugs are designed to overcome pharmaceutical, pharmacokinetic or pharmacodynamics barriers. The prodrug approach can be utilized in several applications: i) some prodrugs are designed to improve the drug's aqueous solubility, and hence bioavailability. Enhancing the aqueous solubility of a drug by improving its dissolution rate can be achieved by linking the parent drug to polar or ionizable functional groups like phosphates, amino acids, or sugar moieties. This strategy is useful in parenteral or injectable drug delivery as well [86, 87].

ii) Prodrugs are most commonly applied to enhance the oral and/or topical permeability and absorption of drugs through biological membranes, by increasing the lipophilicity of drugs *via* masking polar and ionizable groups. Linking hydrophilic moieties like hydroxyl, carboxyl, thiol, phosphate, or amine groups with lipophilic linkers can significantly enhance permeability by passive transport [88]. Moreover, intestinal absorption or brain delivery can be enhanced by targeting carrier mediated transporters, which is done by designing prodrugs that mimic the substrates of such transporters [89, 90].

iii) Prodrugs can be made to enhance the organoleptic properties of active drugs, most commonly for taste masking. Agreeable drug taste is an important factor for drug compliance, especially in the pediatric population. For that, bad or bitter taste of drugs can be eliminated by masking the drug's functional groups that bind to taste receptors, or by reducing the solubility of drugs in saliva [91].

iv) In some cases, prodrugs are designed to improve drugs metabolism. Some drugs are subject to first pass metabolism in the liver and/ or the gastrointestinal tract, which decreases the systemic

availability of these drugs. This can be resisted by masking the essential functional groups that are vulnerable to metabolism [92].

v) The prodrug approach is among the most promising site-selective strategies. Site selectivity is important for increasing the therapeutic activity of drugs and lowering toxicity, this is especially useful in chemotherapy drugs for tumor selectivity. Directed enzyme prodrug therapy (DEPT) is an example of prodrug targeted delivery, where it exploits specific artificially introduced enzymes to activate prodrugs in the desired location within the body. The prodrug activating enzyme may be linked to an antibody that is designed against specific tumor antigen (Antibody-directed enzyme prodrug therapy (ADEPT)), or encoded by gene vectors that are capable of targeting cancer cells (Gene-directed enzyme prodrug therapy (GDEPT)). A special type pf GDEPT is Virus-directed enzyme prodrug therapy (VDEPT), in which viral vectors are used to carry the gene of the prodrug activating enzyme [93-95].

1.3.2. Enzyme models used in prodrug design

For prodrugs to be activated, they must undergo either enzymatic or nonenzymatic (chemical) conversion to their parent drugs. Enzymatically activated prodrugs are meant to be converted to the active drug *via* intermolecular reactions with enzymes, like esterases and amidases. This type of prodrugs may have interpatient variability, as enzymatic activity is affected by genetic polymorphism, age, gender, health, and drug interactions [96]. On the other hand, enzymes are known for their magnificent efficiency in reaction catalysis. It is estimated that enzymes accelerate reaction rates 5 - 17 orders of magnitude, compared with uncatalyzed transformations in aqueous solutions [97]. Enzymes catalyze reactions by bringing together and orienting substrates in a conformation that allows the conversion of the substrate to the transition state with minimum

energy [98]. In an attempt to mimic enzyme catalysis, many scientists have explored mechanisms of enzyme catalysis and presented enzyme models in which intramolecular processes can proceed faster than their intermolecular counterparts [99].

Among enzyme models of which their mechanisms were investigated is the model presented by Bruice and coworkers of the nucleophilic cyclization reaction of dicarboxylic semi-esters to anhydrides [100] (illustrated in **Figure 1.3**). Bruice *et al.* showed that the rate of anhydride formation is highly accelerated upon the intramolecular ring-closing reaction of a dicarboxylic semi-ester when compared to its bimolecular counterparts, and the acceleration is driven mainly by enthalpic effects as a result of the proximity of the nucleophile to the electrophile in the ground state molecules [101, 102]. Bruice and Lightstone introduced the term near attack conformation (NAC) to define the required conformation for juxtaposed reactants to enter a transition state. The rate constant of the intramolecular reaction is proportional to the mole fraction of reactant conformations present as the NAC [103].

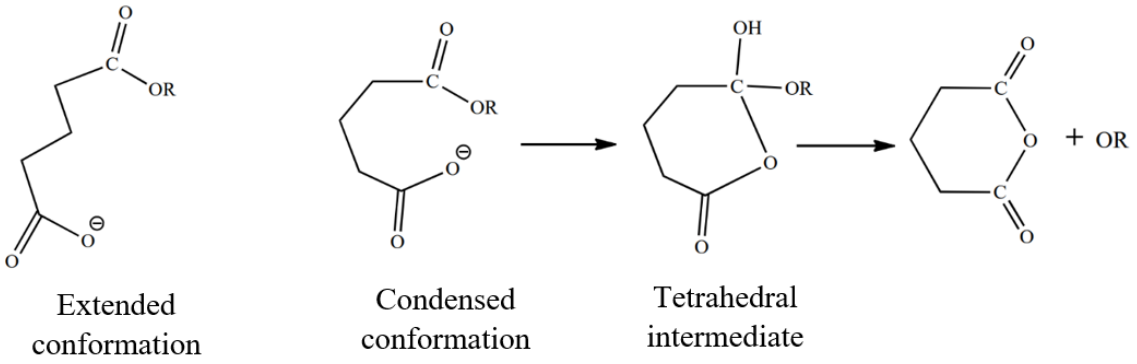

Figure 1. 3: Illustration of intramolecular nucleophilic catalysis of ester hydrolysis of Bruice's enzyme model. The distance between the nucleophile ($O^-$of COO^-) and the electrophile (C of COOR) in the condensed conformation is shorter than that of the extended conformation, and thus the cyclization will be more efficient.

Other driving forces responsible for intramolecular reaction acceleration, that were proposed as enzyme models, include: the acid-catalyzed lactonization of the trimethyl-lock system and other hydroxycarboxylic acids studied by Cohen and Milstien [104], the intramolecular proton-transfer from oxygen to carbon, and between two oxygens in some rigid systems studied by Menger [105], the SN_2-based ring-closing reactions investigated by Brown and Mandolini [106, 107], the proton transfer between two oxygen atoms and between nitrogen and oxygen in some of Kirby's acetals [108, 109], and the acid-catalyzed hydrolysis of N-alkylmaleamic acid derivatives studied by Kirby [110].

In the era of advanced technology, various computational methodologies are available that can be used to model the structures and dynamics of enzymes, and elucidate the detailed mechanisms of enzymatic reactions. Molecular mechanics (MM), such as ab initio, semi-empirical, and density functional theory (DFT) and quantum mechanical (QM) methods are among the most used computational methods for providing structure-energy calculations [99]. These calculations can be applied for the prediction of potential prodrugs. Karaman and coworkers have reported several novel prodrug designs based on computational studies exploring different enzyme models using a variety of molecular orbital and MM methods, and correlations between experimental and calculated rate values for some intramolecular processes. Their studies revealed that both entropy and enthalpy affect the rate of acceleration for intramolecular reactions[111-116]. Unlike Bruice's findings, Karaman's calculations of the kinetic properties of Bruice's enzyme models indicated that the rate enhancement in the cyclization of di-carboxylic semi-esters is the result of strain effects only and not proximity orientation. Meaning that if an intramolecular system is significantly strained and the strain is relieved when arriving at a transition state, then an

intramolecular reaction is expected to be faster than the corresponding intermolecular reaction [117, 118].

All the research on enzyme models has facilitated the design of prodrugs that can be chemically activated by intramolecular reactions solely, *via* the implementation of enzyme models as prodrug linkers. By this approach, the active drug release rate will be entirely dependent on the structural features of the linker attached to the active drug. Utilization of this prodrug approach eliminates disadvantages associated with prodrug activation by metabolic enzymes.

1.4. Problem statement

Atorvastatin is one of the first-line treatments of hypercholesterolemia and related consequences. Atorvastatin has the shortcoming of low oral bioavailability (14%), due to extensive presystemic clearance in the intestines and first pass metabolism in the liver. Because of this problem, high doses of atorvastatin must be administered to attain the required pharmacological effect, despite the fact that atorvastatin has high intestinal permeability and high potency. High doses of atorvastatin entering the body, and thus high concentrations of metabolites, are responsible for a number of adverse effects that are dose related. The most considerable adverse effects are the statin-induced myopathies that include the life-threatening rhabdomyolysis. Treatment of atorvastatin is life long, therefore, such drug must be safe and well tolerated.

For that, there is a need to modify the metabolic profile of atorvastatin in a manner that enables the administration of lower doses of atorvastatin to get the required pharmacological effect with the least possible risk of adverse effects. And given that the prodrug approach is superior in improving drug properties, including high metabolic lability, it was used in this research to resolve the shortcoming of atorvastatin's bioavailability. Though this is not the first time that the prodrug

approach is explored with atorvastatin; this, to the best of our knowledge, is the first work to synthesize and study chemically activated atorvastatin prodrugs. knowing that chemically activated prodrugs outweigh enzymatically activated prodrugs, in which the former has better-predictable pharmacological and toxicological effects.

1.5. Objectives

The general objective of this research was to synthesize and evaluate novel prodrugs of atorvastatin that improve atorvastatin bioavailability by decreasing presystemic metabolism. It was intended to synthesize prodrugs of atorvastatin by an esterification reaction that links anhydride molecules (Bruice's enzyme models) to the 3, 5 hydroxyl groups of atorvastatin, to produce ester prodrugs which can be hydrolyzed in aqueous media to the parent drug (atorvastatin) and a non-toxic moiety (the anhydride linker) *via* intramolecular chemical hydrolysis. By masking the metabolic labile hydroxyl groups of atorvastatin, the prodrugs are supposed to have lower susceptibility for presystemic clearance, and hence higher bioavailability. Moreover, linking hydrophilic groups to the structure of atorvastatin is expected to enhance water solubility and afford moderate hydrophilic lipophilic balance (HLB) value.

Specific objectives were:

- To synthesize atorvastatin prodrugs using the linkers of maleic anhydride, succinic anhydride, and phthalic anhydride.
- To characterize the new prodrugs by melting point, FT-IR, LC-MS and ^{1}H-NMR spectroscopy.
- To study the *in vitro* conversion kinetics of the new prodrugs in a pH range of 1-7.4.

1.6. Research questions

1. Is it possible to link atorvastatin to anhydride linkers *via* chemical synthesis?
2. Do the synthesized atorvastatin prodrugs have physiochemical properties which could lead to high bioavailability?
3. Will the synthesized prodrugs be able to chemically release atorvastatin in a programmable manner?
4. Do the synthesized atorvastatin prodrugs have the potential to be used in several dosage forms?

Chapter Two

Literature Review

2. Chapter 2. Literature review

The essence of this work is based on two segments; the first one is the bioavailability enhancement of atorvastatin, and the second is the utilization of enzyme models for prodrug formation. So, this chapter provides a brief review of the literature regarding these two topics.

2.1. Literature review on bioavailability enhancement of atorvastatin

The low bioavailability of atorvastatin is a problem that attracted the interest of many researchers, and many attempts to overcome this problem were pursued using different strategies. There is a number of studies that followed the approach of formulation improvement in order to increase the solubility and dissolution, and so the bioavailability of atorvastatin, while other studies considered the preparation of prodrugs to enhance the absorption of the drug.

2.1.1. Improved formulations of atorvastatin

A variety of strategies that involve the use of solubilizers and micronization/nanosizing have been reported in the literature for improving the solubility and dissolution rate of atorvastatin. To optimize the kinetic profile of atorvastatin, Hashem *et al.* have developed an atorvastatin–zein nanosphere formula (zein polymer). The zein polymer is composed of a group of alcohol-soluble proteins and is used as a drug delivery vehicle. Loading atorvastatin on zein particles resulted in increased bioavailability of 3 folds of that of conventional atorvastatin when tested *in vivo* in rats [119]. The same research team have developed two formulas of atorvastatin in self-nanoemulsifying drug delivery system (SNEDDS) and solid nano-suspension (NS), in order to enhance the dissolution characters of atorvastatin. The SNEDDS was formulated using the solubilizers of oleic acid, Tween 80 (surfactant), and propylene glycol. The NS was formulated by

the antisolvent precipitation–ultrasonication method. The formulation of SNEDDS showed superior improvement in pharmacokinetic parameters and bioavailability compared with the NS formula. Bioavailability estimation in rats revealed that SNEDDS and NS formulae improved the bioavailability of atorvastatin by 93.81% and 55.31%, respectively, relative to atorvastatin suspension and the conventional tablets [120].

Khan *et al*. [121] presented an oral nanostructured lipid carrier formulation of atorvastatin. The optimized formulation was composed of oleic acid and stearic acid as lipid phase, poloxamer 188 as surfactant and chlorogenic acid (an excipient having synergistic cholesterol lowering activity). The plasma concentration time profile of atorvastatin in rats showed 3.08- and 4.89-fold increase in relative bioavailability of the new formulation with respect to conventional tablets and drug suspension, respectively.

Jain *et al.* formulated atorvastatin as an oil-in-water nano-emulsion. This work aimed to increase the solubility of atorvastatin and hence its bioavailability. The formulation used for the assessment of the bioavailability contained 15% of oil (oleic acid). The absorption of atorvastatin from nano-emulsion resulted in 2.87- and 2.38-fold increase in bioavailability as compared to conventional tablets and pure drug suspension respectively [122].

For enhancing the dissolution rate of atorvastatin calcium, Mei Yin *et al.* prepared atorvastatin calcium dry emulsion using the spray drying method. Dry emulsion formulations are typically prepared from oil in water (o/w) emulsions containing a soluble or insoluble solid carrier in the aqueous phase by spray drying, lyophilization, or evaporation. In this study PlurolOleique CC 497 was used as an oil phase. The *in vitro* intestinal absorption of atorvastatin calcium from the dry emulsion formulation showed a 2.33-fold increase compared to the pure unformulated atorvastatin

calcium powder [123]. Another dry emulsion formulation of atorvastatin was prepared by Salama *et al*. [124]. In this formulation, the dry emulsion was prepared by lyophilization of o/w emulsion of atorvastatin using Labrafac as the oil phase in the presence of surfactant. *In vitro* dissolution study revealed enhanced dissolution rate of atorvastatin from the lyophilized dry emulsion tablets compared to the plain drug.

Another attempt to increase atorvastatin's bioavailability was by forming stabilized gastro-retentive floating tablets of atorvastatin by Khan *et al*. The study suggested that the low bioavailability of atorvastatin is attributed to incomplete absorption, so a stabilized floating tablet formulation was created. A release retarding polymer (HPMC K15M) was used in the formula of the tablets. The formulation gave floating lag time of 56±4.16 s and good matrix integrity with *in vitro* dissolution of 98.2% in 12 h. *In vivo* pharmacokinetic study revealed enhanced bioavailability of floating tablets about 1.6 times compared with that of the conventional tablet [125].

Most of the improved formulations of atorvastatin reported in literature are deficient in comprehensive details of pharmacokinetic, pharmacodynamic and safety profile. Additionally, formulations containing high amounts of solubilizers, like self-emulsifying formulations are not always safe [126]. Moreover, these formulations have issues that may limit their clinical translation, like expensive and complex manufacturing steps, poor drug loading capacity, premature drug release, and biocompatibility and biodegradability of carrier materials. Most importantly, although the results of the studies showed some improvement in the bioavailability of atorvastatin, these results, which are extrapolated from *in vivo* experiments in rats, are subject to be irrelevant to humans; since humans differ from animals regarding isoform composition,

expression and catalytic activity of drug-metabolizing enzymes. In particular, rats lack CYP3A4, the isoenzyme responsible for atorvastatin metabolism in humans [127].

2.1.2. Prodrugs of atorvastatin

Mizoi *et al.* aimed to enhance the bioavailability of atorvastatin by increasing its lipophilicity and absorption. The synthesized atorvastatin esters have the potential to be prodrugs *in vivo*. The prodrugs were prepared by esterification of the carboxylic acid moiety of atorvastatin using eleven different alcohols. The results were eleven kinds of esters that were metabolized by human carboxylesterases *in vitro*, mainly by CES1 isoenzyme [128]. **Figure 2.1** presents the structure of the best three candidates for the synthesized prodrugs.

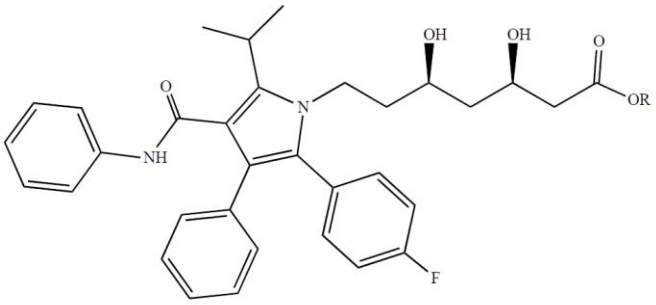

1.R= CH_3

2.R= Allyl

3.R= p-F-Ph

Figure 2. 1: Chemical structures of atorvastatin esters synthesized by Mizoi *et al* [128].

Immadi *et al* attempted to improve the absorption of atorvastatin by transdermal administration of atorvastatin prodrugs. They prepared atorvastatin ethyl ester **(Figure 2.2)** and formulated the prodrug in an adhesive transdermal delivery system matrix. Transdermal atorvastatin prodrug showed a high *in vitro* permeation rate. More than 50% of the penetrated prodrug was hydrolyzed to atorvastatin by the esterase enzyme in the skin after permeation *in vitro* [129].

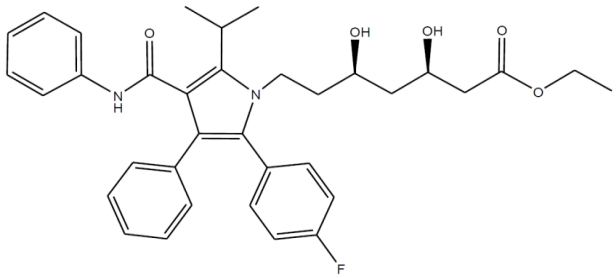

Figure 2. 2: Chemical structure of atorvastatin ethyl ester synthesized by Immadi *et al.* [129]

Atorvastatin ester prodrugs are dependent on enzymatic activation, which is variable among individuals or even in the same individual, leading to variable drug bioavailability. Also in these prodrugs, the linker is linked to the carboxylic acid end, masking an important participant moiety for water solubility.

By reviewing the literature, it can be observed that almost all the studies aimed to enhance atorvastatin bioavailability by increasing its aqueous solubility. None of the previous research on novel formulations nor novel prodrugs did treat the primary cause of the low bioavailability, which is the extensive metabolism in the gut wall and the liver.

2.2. Literature review on prodrug design based on enzyme models

Modern prodrug approaches are based on intramolecular processes using computational methods and correlations between experimental and calculated values to design linkers to be covalently attached to the active drug. Karaman Group has worked on the design of innovative prodrugs with higher bioavailability for drugs containing hydroxyl, amine, or phenol groups using modern computational methods. Statins were among these drugs. Simvastatin has a low aqueous solubility and low bioavailability (5%) due to slow tissue penetration and consequently extensive first pass effect. Therefore, improving its solubility and dissolution rate is essential to enhance its

bioavailability. Karaman *et al*. proposed three approaches of prodrugs to increase statin bioavailability using Kirby's enzyme models and Bruice's enzyme model as linkers for simvastatin **(Figure 2.3)**. This has led to the design of three simvastatin prodrugs based on proton transfers in Kirby's enzyme model by linking the free hydroxyl group of simvastatin to an amine linker (Kirby's enzyme model). The designed prodrugs are more hydrophilic and have the potential to provide simvastatin with higher bioavailability [130].

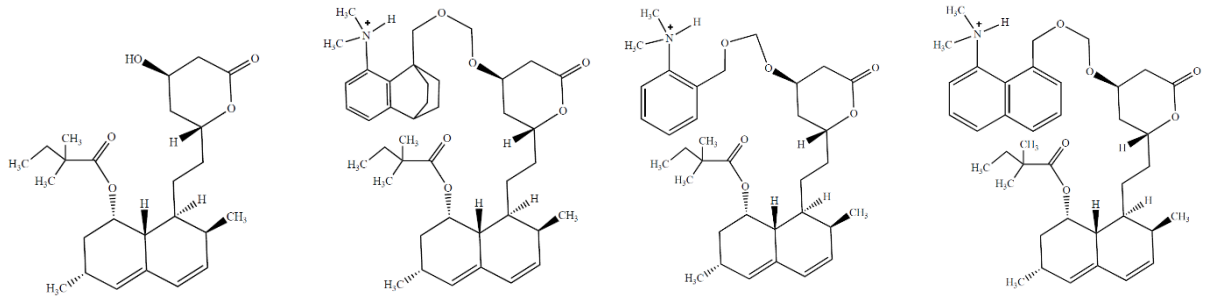

Simvastatin | Simvastatin prodrug 1 | Simvastatin prodrug 2 | Simvastatin prodrug 3

Figure 2. 3: Chemical structures of simvastatin and simvastatin prodrugs designed by Karaman *et al.* [130].

Investigations of Bruice's theory of proximity orientation by Ab initio and DFT calculations indicated that the remarkable acceleration in the cyclization of the di-carboxylic semi-esters is solely the result of a strain effect [117]. Exploring the mechanism of Bruice's cyclization of dicarboxylic semi-esters enzyme model has led to the design and synthesis of novel prodrugs of the antimalarial atovaquone, with better bioavailability than the active drug, atovaquone. In these prodrugs, a di-carboxylic semi-ester linker was linked to the hydroxyl group of atovaquone to form a system with higher hydrophilicity and water solubility than its parent drug and is able to release atovaquone in a chemically driven controlled manner [118, 131].

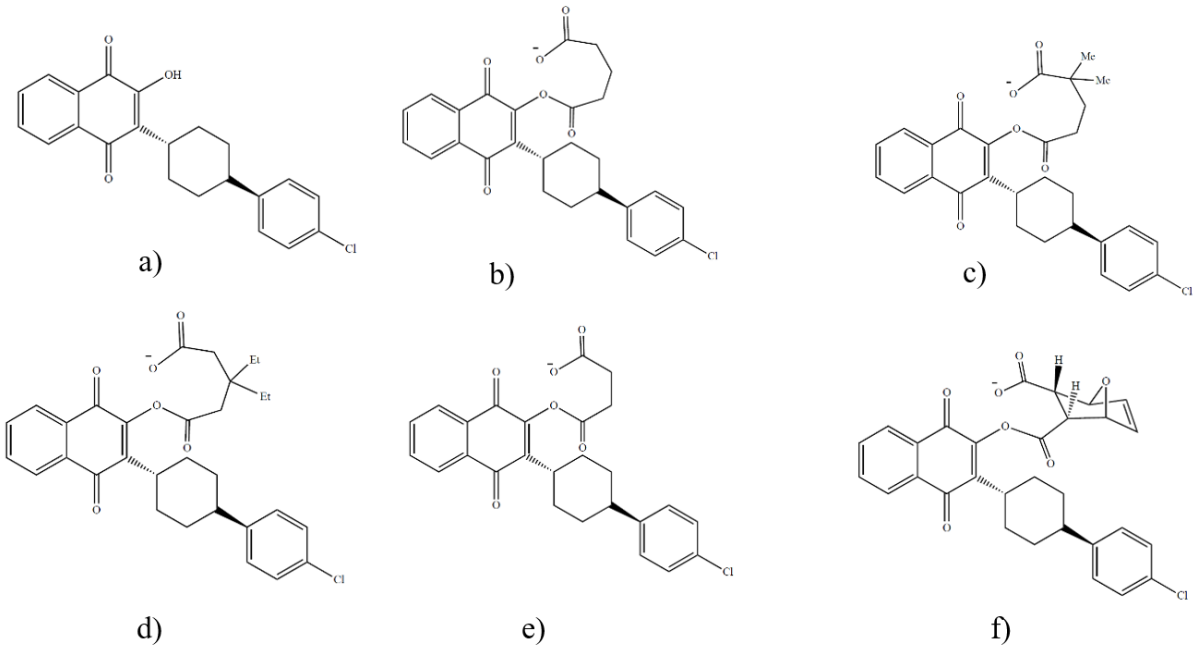

Figure 2. 4: Chemical structures of atovaquone (a) and atovaquone prodrugs (b-f) proposed by Karaman *et al*. [118].

In addition, by studying the mechanism of intramolecular acid-catalyzed hydrolysis of Kirby's N-alkylmaleamic acids, and proton transfers between two oxygens in Kirby's acetals, different promoieties were utilized for the design and synthesis of a number of prodrugs with enhanced dissolution, membrane penetration, and bioavailability. These include novel prodrugs of tranexamic acid to treat bleeding conditions [132], acyclovir as an antiviral drug [133], atenolol to treat hypertension [134, 135], dimethyl fumarate for the treatment of psoriasis [136], phenylephrine as a decongestant [137], cefuroxime as an antibiotic [137], and aza-nucleosides for the treatment of myelodysplastic syndromes [138]. Menger's kemp acid enzyme model was also utilized for the design and synthesis of dopamine prodrugs for the treatment of Parkinson's disease [139].

Moreover, different promoieties were used for the design and synthesis of prodrugs for masking the bitter taste of some drugs, such as paracetamol, atenolol, cefuroxime, amoxicillin, and

cephalosporins; synthesized to enable the formulation in aqueous preparations without experiencing bad taste [140-142]. Prodrug linkers were used to block the free amine or phenol groups, which are responsible for the drug bitterness, and to enable the release of the parent drug in a controlled manner [143].

The results of the previous studies demonstrated that the rate by which the prodrug releases the active drug can be determined according to the structural features of the prodrug promoiety (the enzyme model). In view of the findings of the previous research on enzyme models and intramolecularity, three prodrugs of atorvastatin were proposed in which the prodrug promoiety is a di-carboxylic semi-ester (Bruice's enzyme model). The prodrugs are designed to be activated by intraconversion, which is the result of cyclization of the prodrug promoiety (the anhydride) as illustrated in **Scheme 1**.

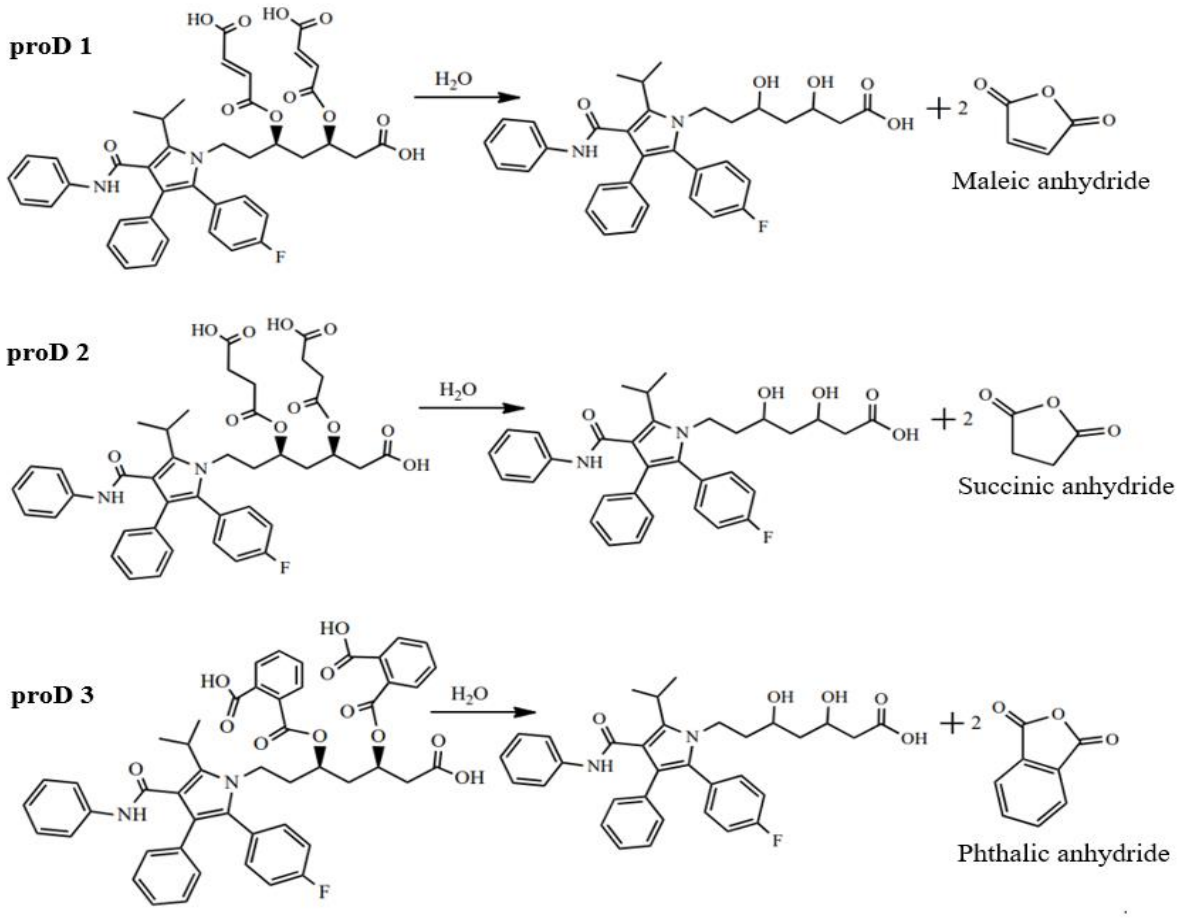

Scheme 1: Intraconversion of atorvastatin prodrugs to atorvastatin *via* cyclization.

Chapter Three

Experimental

3. Chapter 3: Experimental

3.1. Materials

Atorvastatin calcium pure standard was supplied by Pharmacare PLC, succinic anhydride, maleic anhydride, phthalic anhydride, sodium hydride, sodium hydroxide, monobasic sodium phosphate, sodium phosphate dibasic were all purchased from Sigma-Aldrich.

p-Dioxane was purchased from Avantor Performance Materials, J.T. Baker®. All other solvents were purchased from Sigma Aldrich. Distilled water was obtained from a reverse osmosis purifier available at Al-Quds University-Faculty of Pharmacy labs.

3.2. Analysis of atorvastatin (and prodrugs) by UPLC-UV/Vis

An analytical method for drug identification and quantitation was developed on UPLC-UV/Vis for atorvastatin and each synthesized prodrug. Specifically, Shimadzu's Nexera X2 UPLC system with Shimadzu Prominence SPD-M20A Diode Array Detector and Shimadzu's LabSolutions software was used. Atorvastatin and the prodrugs were separated on a Roc C18 column (100x4.6mm, 3 microns). The mobile phase used was a methanol: phosphate buffer (pH 7) mixture (70:30, v/v) with a flow rate of 1 mL/min. the detection wavelength ($\lambda_{Detection}$) was 244 nm. All the UPLC analysis in the following sections were performed using this method.

3.3. Prodrugs synthesis and characterization

3.3.1. Synthesis and characterization of atorvastatin ProD1

Atorvastatin calcium (577mg, 0.5 mmol and equivalent to 1 mmol of atorvastatin) was dissolved in 50 mL of anhydrous dioxane, to which sodium hydride (150 mg) was added. The mixture was stirred at 50℃ . After 30 minutes of stirring, maleic anhydride (294mg, 3 mmol) was added to the

reaction mixture, and the mixture was refluxed with stirring and heating at 65 ℃. The reaction progress was monitored by the disappearance of atorvastatin, which was determined by UPLC analysis of samples withdrawn from the reaction mixture over time. After one hour, the reaction was complete and the reaction flask was cooled in an ice bath. Then the solvent was evaporated under reduced pressure, and a pink precipitate was collected. The crude product was washed with hexane and ethyl acetate, and then it was left to completely dry in an oven at 37 ℃ for 24 hours. Thereafter, the product was characterized by melting point, FT-IR spectroscopy, ^{1}H NMR and positive electrospray ionization mass spectrometry (ESI-MS).

The Fourier transform infrared (FT-IR) spectra were recorded on a Bruker FT-IR spectrometer equipped with a platinum attenuated total reflectance (ATR) unit. The LCMS analysis was conducted using a Thermo Fisher scientific UPLC-MSMS system in the positive electrospray ionization (+ESI) mode. ^{1}H-NMR spectra were recorded on a Varian NMR spectrometer (400 MHz).

% Yield = 93%; ^{1}H-NMR (400 MHz, D_2O) δ ppm: 1.4 (dd, 6H), 1.7 (m, 2H), 1.85 (m, 2H), 1.9 (m, 2H), 2.39 (m, 1H), 2.5 (m, 1H), 3.3 (m, 1H), 3.7 (s, 1H), 4 (t, 2H), 5.7 (d, 1H), 5.8 (d, 1H), 6.58-6.62 (dd, 2H), 7.18-7.23 (m, 10H), 7.3-7.4 (m, 4H).

3.3.2. Synthesis and characterization of atorvastatin ProD2

The same procedure of synthesis and characterization of atorvastatin ProD1 was followed, but succinic anhydride (300 mg, 3 mmol) was used as the linker instead of maleic anhydride. The product of the synthesis was an off-white powder.

% Yield = 93%; ^{1}H-NMR (400 MHz, D_2O) δ ppm: 1.4 (d, 6H), 1.7 (m, 2H), 1.8 (m, 2H), 1.9 (m, 2H), 2.3-2.5 (d, 8H), 2.55 (m, 2H), 3.3 (m, 1H), 3.76 (s, 1H), 4 (t, 2H), 7.17-7.23 (dd, 10H), 7.36-7.38 (t, 4H).

3.3.3. Synthesis and characterization of atorvastatin ProD3

The same procedure of synthesis and characterization of atorvastatin ProD1 and ProD2 was followed for ProD3 synthesis, except that phthalic anhydride (444 mg, 3 mmol) was used as the linker. The synthesis yielded a white powder.

% Yield = 92%; ^{1}H-NMR (400 MHz, D_2O) δ ppm: 1.34-1.4 (dd, 6H), 1.94-2.05 (m, 2H), 2.1 (m, 2H), 2.2 (m, 2H), 2.5 (m, 1H), 2.7 (m, 1H), 3.3 (m, 1H), 3.77 (s, 1H), 4.09 (t, 2H), 6.90-6.94 (t, 2H), 7 (d, 2H), 7.14-7.25 (m, 7H), 7.36-7.50 (m, 8H), 7.54-7.64 (m, 3H).

3.4. kinetic study of prodrugs *in vitro* degradation

3.4.1. Calibration curve construction

Linear standard curves were used for quantitation of the synthesized prodrugs and atorvastatin using the UPLC-UV/Vis method mentioned in section 3.2. All compounds were quantified by comparing peak areas to known standards (1000-125 ppm) generating linear standard curves.

3.4.2. Hydrolysis media preparation

Phosphate buffer (50mM) was prepared by dissolving monobasic sodium phosphate in distilled water. From that solution, separate portions were adjusted to pH of 6.8 and 3, using concentrated phosphoric acid and 1M sodium hydroxide (NaOH) solution.

0.1N acid solution was prepared by diluting concentrated hydrochloric acid (HCl) solution (37%) with distilled water.

For prodrug plasma hydrolysis, human blood plasma was centrifuged twice and the supernatant was collected to be used as a solvent.

3.4.3. *In vitro* prodrug intraconversion kinetic study

Three solutions of atorvastatin standard in a concentration of 500 ppm were prepared by dissolving atorvastatin in 0.1N HCl solution, phosphate buffer pH 3, and phosphate buffer pH 6.8. Each solution was analyzed by UPLC to detect atorvastatin's retention time. Similar solutions were prepared using atorvastatin ProD1, ProD2, and ProD3. For prodrug plasma hydrolysis, each prodrug was dissolved in plasma at a concentration of 500 ppm. All the prodrug solutions were incubated in a water-bath at 37℃, and samples of each solution were analyzed by UPLC over time. Plasma samples were prepared by diluting plasma with water in a 1:1 ratio and filtration. The progression of each prodrug conversion in each medium was followed by monitoring the disappearance of the prodrugs and the appearance of atorvastatin and the free linkers. Afterward, the data collected was used to calculate the half-life ($t_{1/2}$) of each prodrug.

Chapter Four

Results and Discussion

4. Chapter 4: Results and discussion

4.1. Synthesis of atorvastatin prodrugs

Three novel atorvastatin prodrugs were successfully synthesized by an esterification reaction that conjugates two anhydride moieties to the β and δ hydroxyl groups of atorvastatin **(Scheme 2)**. The reaction results from a nucleophilic attack of the hydroxyl oxygen of atorvastatin at the carbonyl of the anhydride, resulting in conjugation and opening of the anhydride cycle. Atorvastatin prodrug 1 **(proD1, Figure 4.1.a)**, atorvastatin prodrug 2 **(proD2, Figure 4.1.b)** and atorvastatin prodrug 3 **(proD3, Figure 4.1.c)** were synthesized using maleic anhydride, succinic anhydride, and phthalic anhydride as the prodrug linkers, respectively. All the prodrugs were yielded as sodium salts, as a result of the presence of sodium ions, released from sodium hydride (NaH), in the reaction mixture. It was important to add NaH to the reaction pot long enough before the addition of the anhydrides; this was to allow the hydride to react with all remnant water molecules in the solvent, to prevent the anhydrides from reacting with water. Moreover, the hydride helped in deprotonating the hydroxyl groups of atorvastatin, increasing their nucleophilicity. To prevent obtaining the product as a mixture of mono- and di-esterified prodrugs, excess amount of the anhydride linker (3eq) was used in the reaction. This resulted in high yield synthesis of pure products.

The final products were in powder forms: ProD1 is a pink powder that melts at 215℃, proD2 is an off-white powder that is decomposed at 230 ℃, and proD3 is a white powder with a melting point of 128 ℃. The three powders have high water solubility, and they lack the profound bitter taste of atorvastatin.

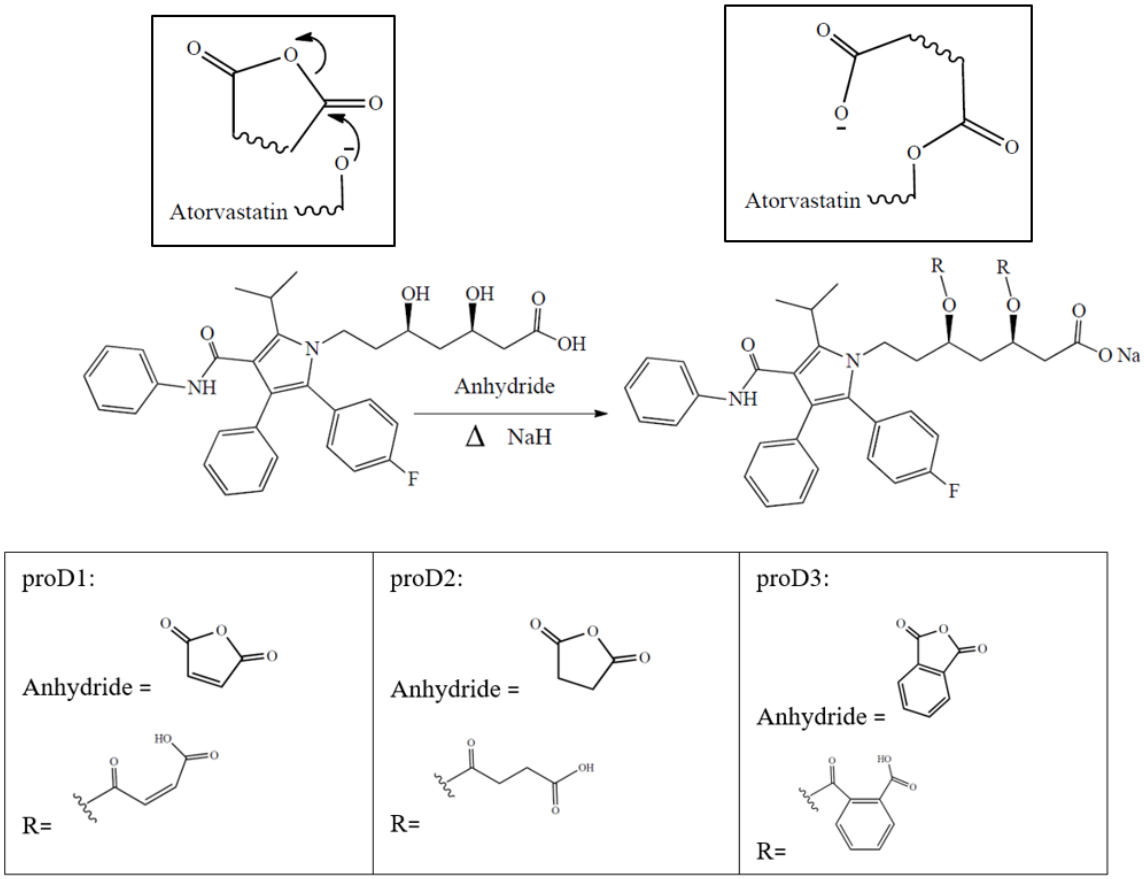

Scheme 2: Reaction of atorvastatin with different anhydrides for the synthesis of atorvastatin proD1, proD2, and proD3.

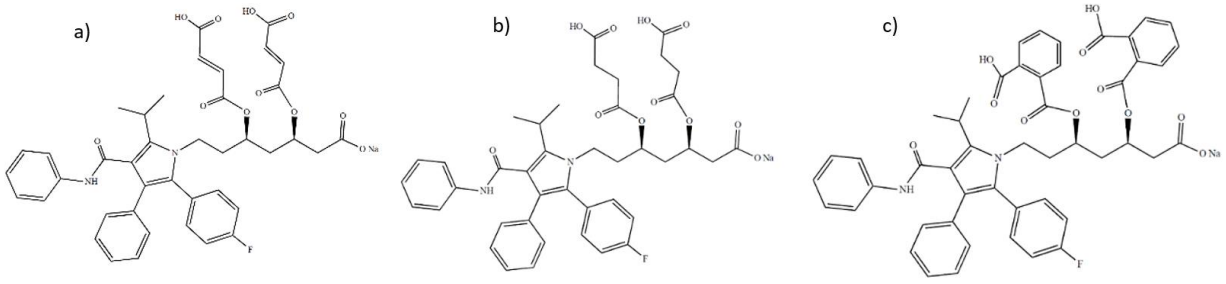

Figure 4. 1: Chemical structures of proD1 (a), proD2 (b), and proD3 (c)

4.2.Characterization of atorvastatin standard

The atorvastatin standard, which was used in the prodrugs' synthesis, was characterized in the same manner as the prodrugs, in order to enable a comparison between the reactant and product of the synthesis. The melting point of atorvastatin is 170 ℃. Figure 4.2 shows the chemical characterization of atorvastatin.

FT-IR spectrum of atorvastatin showed bands at 1509, 1578, 1649, 3237, and 3362 cm^{-1} representing the aromatic C=C, carboxylate carbonyl, amide carbonyl, hydroxyl, and NH stretches, respectively **(Figure 4.2.a)**. Positive electrospray ionization mass spectrometry (+ESI-MS) analysis of atorvastatin acid (M.W= 558.6 g/mol) generated a strong signal for atorvastatin at 559.4 m/z **(Figure 4.2.b)**. Atorvastatin salt was detected by UPLC-UV/Vis at a retention time of 3.25 minutes for ionized atorvastatin **(Figure 4.2.c)**, and atorvastatin acid produced two peaks at 5.3 minutes for atorvastatin free hydroxyl acid and 6.9 minutes for atorvastatin lactone **(Figure 4.2.d)**.

Atorvastatin: ^{1}H-NMR (400 MHz, DMSOD6) δ ppm: 1.4 (6H, $C\underline{H}_3$-CH), 1.6 (2H, CH-$C\underline{H}_2$-CH), 1.9 (m, 2H, CH_2-$C\underline{H}_2$-CH), 2.1 (2H, CH-$C\underline{H}_2$-C=O), 3.3 (1H, $(CH_2)_2$-$C\underline{H}$-O) 3.5 (1H, $(CH_2)_2$-$C\underline{H}$-O), 3.8 (1H, $(CH_3)_2$-$C\underline{H}$-Ar), 4 (2H, CH_2-$C\underline{H}_2$-N), 7-7.6 (14H, Aromatic H), 9.8 (1H, N$\underline{H}$). **(Figure 4.3)**.

Characterization of the prodrugs, which is detailed in the next sections of this chapter, approved that all the characteristics of atorvastatin is distinct from those of the prodrugs. The reactions were successful in converting atorvastatin to new products.

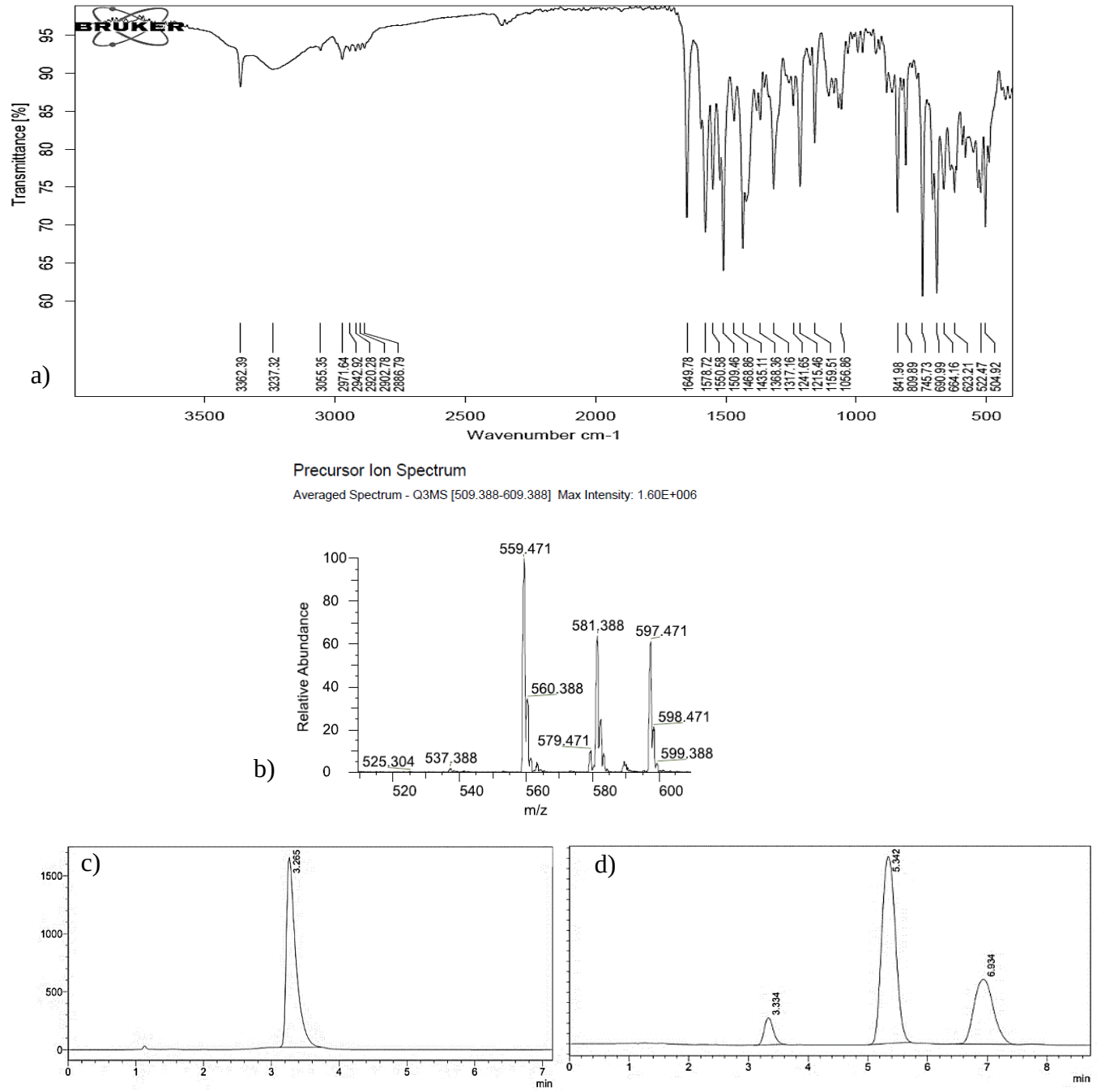

Figure 4. 2: Atorvastatin chemical characterization. FT-IR spectrum of atorvastatin (a). +ESI-MS analysis of atorvastatin acid (b). UPLC detection of atorvastatin salt showing the peak of atorvastatin ionized form (c). UPLC detection of atorvastatin acid showing peaks of the acid form (5.3 min), the lactone form (6.9 min) and the ionized form (3.3 min) (d).

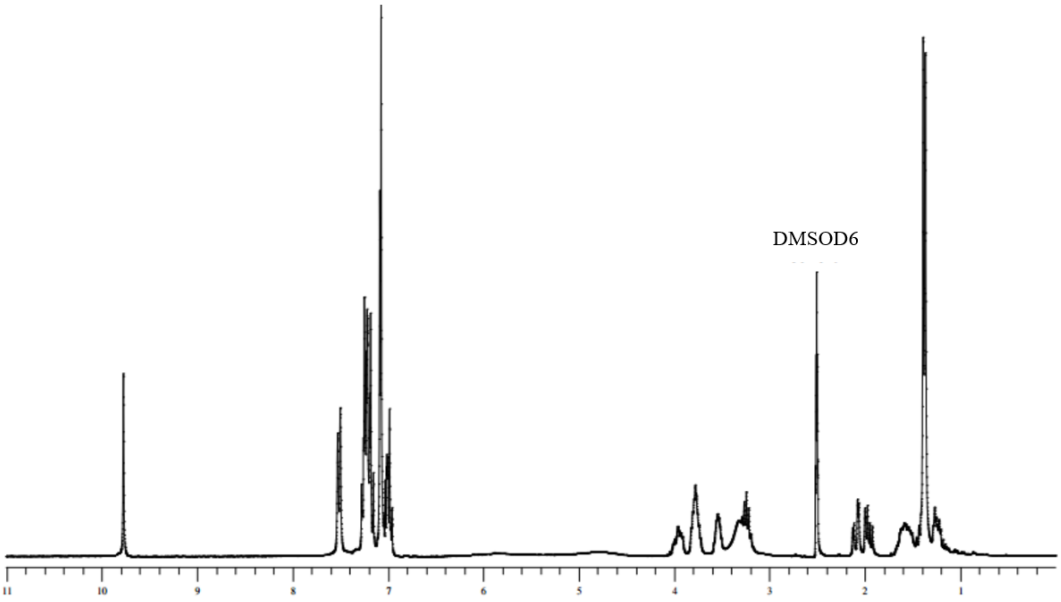

Figure 4. 3: ^{1}H-NMR spectrum of atorvastatin in DMSOD6.

4.3.Characterization of ProD1

ProD1: ^{1}H-NMR (400 MHz, D_2O) δ ppm: 1.4 (dd, 6H, $C\underline{H}_3$-CH), 1.7 (m, 2H, CH-$C\underline{H}_2$-CH), 1.85 (m, 2H, CH_2-$C\underline{H}_2$-CH), 1.9 (m, 2H, CH-$C\underline{H}_2$-C=O), 2.39 (m, 1H, $(CH_2)_2$-C<u>H</u>-O), 2.5 (m, 1H, $(CH_2)_2$-C<u>H</u>-O), 3.3 (m, 1H, $(CH_3)_2$-C<u>H</u>-Ar), 3.7 (s, 1H, N<u>H</u>), 4 (t, 2H, CH_2-$C\underline{H}_2$-N), 5.7 (d, 1H, CH=<u>C</u>H-C=O), 5.8 (d, 1H, CH=<u>C</u>H-C=O), 6.58-6.62 (dd, 2H, CH=<u>C</u>H-C=O), 7.18-7.23 (m, 10H, Aromatic H), 7.3-7.4 (m, 4H, Aromatic H). **(Figure 4.5)**.

Chemical characterization of proD1, including FT-IR spectrum, +ESI-MS spectrum, and UPLC detection, are illustrated in **Figure 4.4.** ProD1 LC-MS analysis **(Figure 4.4.a)** generated a strong signal at 777.4 m/z, which indicates that the product was of a molecular weight of 776.6 g/mol. This result is compatible with the proposed structure of the di-esterified derivative of atorvastatin **(Figure 4.1.a)**. Sodium adduct was also detected at 799.4 m/z. FT-IR was used to further characterize the structure of ProD1 **(Figure 4.4.b)**. Specifically, ProD1 generated absorption band

at 1707 cm^{-1} representing the carbonyl stretch of the ester groups. Additionally, carbonyl absorption at the carboxylate stretch (1557 cm^{-1}) is intensified because of the additional carbonyl groups of the linker. The hydroxyl groups of atorvastatin are masked by ester bonds in the structure of proD1, and different OH bonds (acid OH of the linker) are present. So, the OH band appeared wider and stronger around 3351 cm^{-1}. ^{1}H-NMR confirmed the structure of proD1 as well, signals at 5.7, 5.8, and 6.58-6.62 ppm represent the four protons of the maleic linkers.

ProD1 was detected by UPLC at 1.54 minutes **(Figure 4.4.c)**. The prodrugs have shorter retention times in RP chromatography compared to the parent drug, because they have more polar and ionizable moieties within their structures, which makes them systems of higher hydrophilicity.

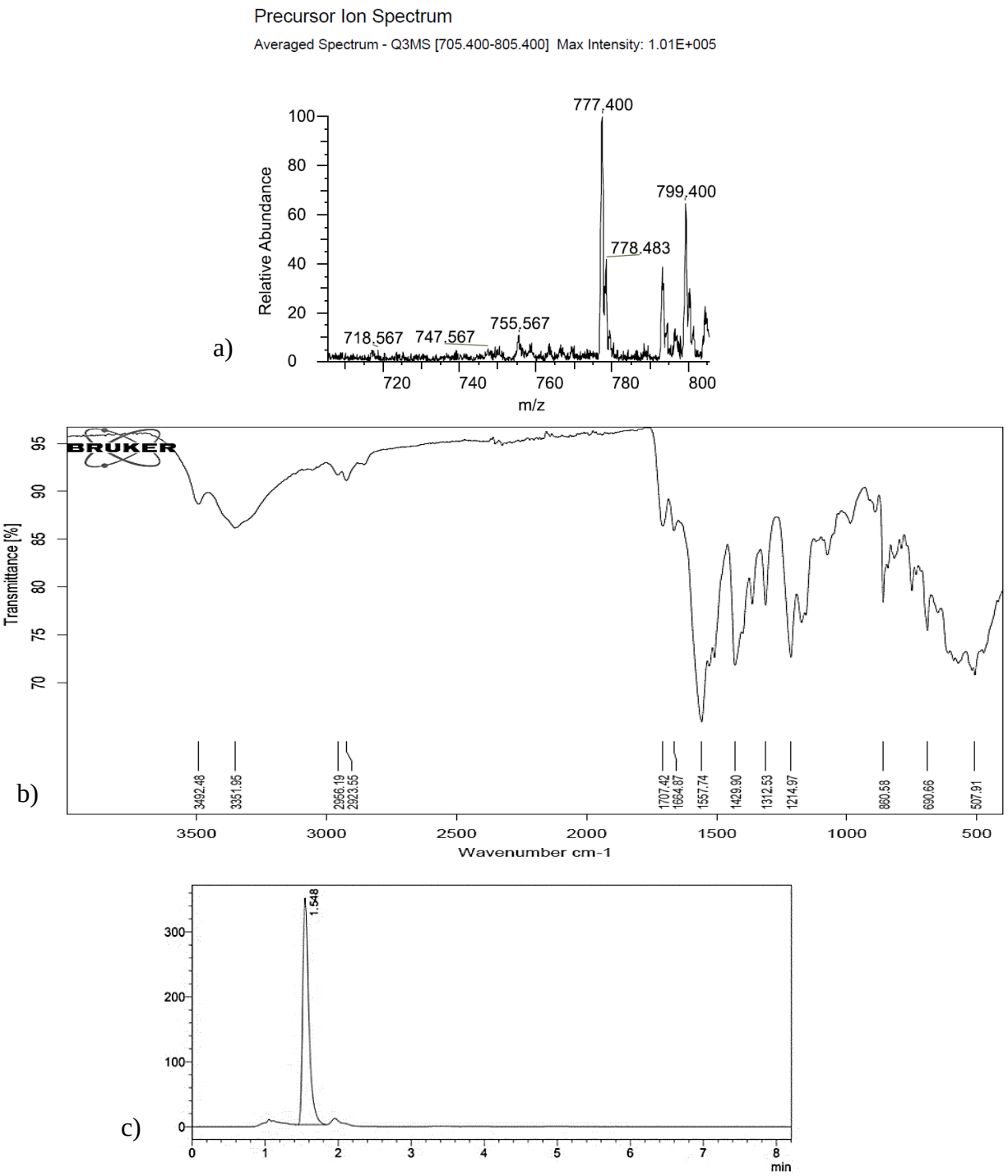

Figure 4. 4: Chemical characterization of proD1. +ESI-MS analysis (a), FT-IR spectrum (b), and UPLC detection (c) of proD1.

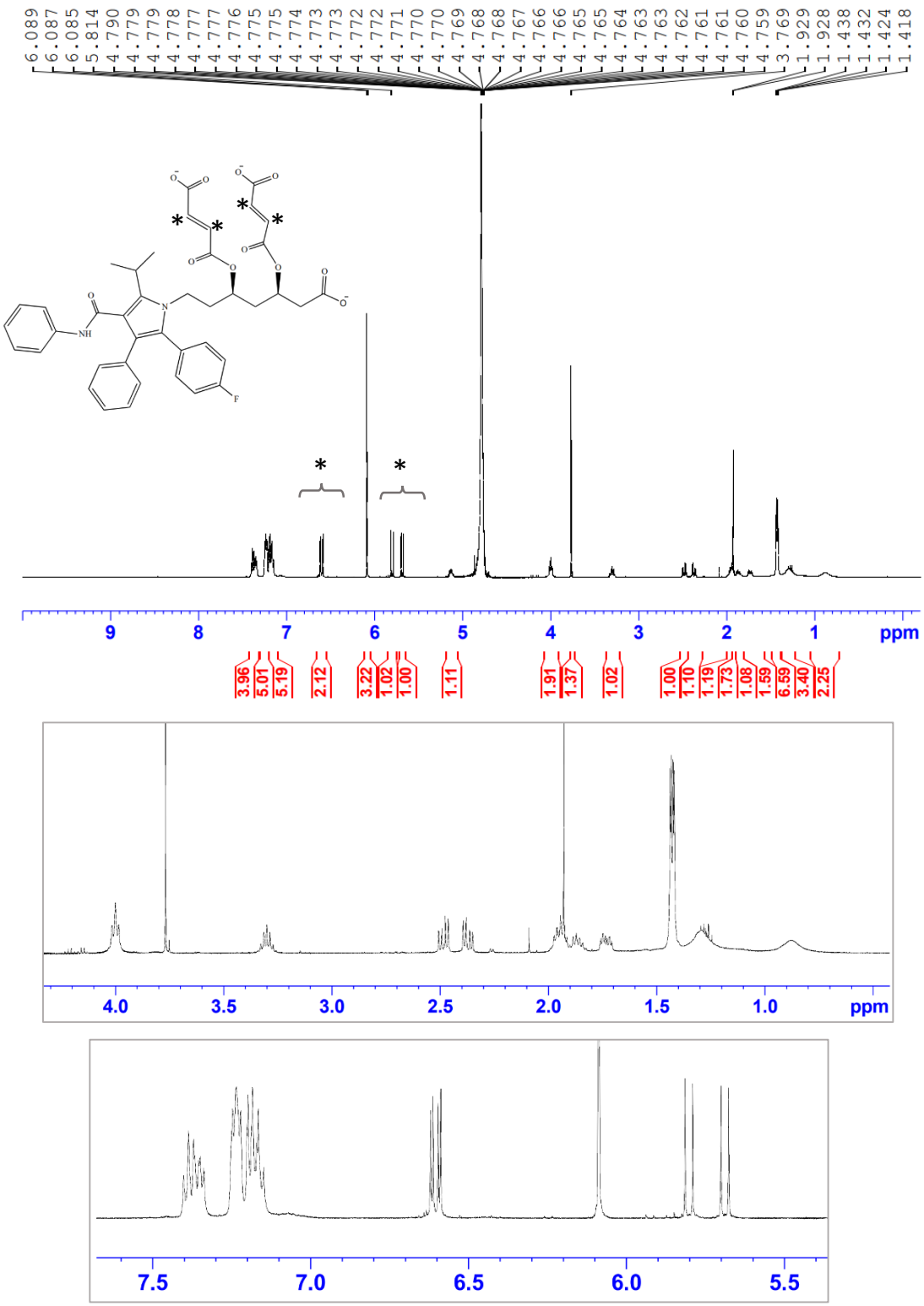

Figure 4. 5: ^{1}H-NMR spectrum of proD1 in D_2O. The protons of the maleate linkers were detected at 5.7, 5.8, and 6.58-6.62 ppm.

4.4.Characterization of ProD2

ProD2: ^{1}H-NMR (400 MHz, D_2O) δ ppm: 1.4 (d, 6H, $C\underline{H}_3$-CH), 1.7 (m, 2H, CH-$C\underline{H}_2$-CH), 1.8 (m, 2H, CH_2-$C\underline{H}_2$-CH), 1.9 (m, 2H, CH-$C\underline{H}_2$-C=O), 2.3-2.5 (d, 8H, CH_2-$\underline{C}H_2$-C=O), 2.55 (m, 2H, $(CH_2)_2$-C$\underline{H}$-O), 3.3 (m, 1H, $(CH_3)_2$-C$\underline{H}$-Ar), 3.76 (s, 1H, N$\underline{H}$), 4 (t, 2H, CH_2-$C\underline{H}_2$-N), 7.17-7.23 (dd, 10H, Aromatic H), 7.36-7.38 (t, 4H, Aromatic H). **(Figure 4.7)**.

^{1}H-NMR confirmed the successful synthesis of proD2, the eight protons of the succinic linkers can be identified at 2.3-2.5 ppm. LC-MS analysis of proD2 generated a strong signal at 781.5 m/z **(Figure 4.6.a)**, which represents the M+1 value of the salt form of the di-succinate prodrug (M.W.= 780.6 g/mol, the structure is illustrated in **Figure 4.1.b**). The spectrum shows a signal at 797.5 m/z, which represents the potassium adduct of the acid form of the prodrug. When the prodrug is dissolved in methanol (which is the solvent used for sample preparation in the LCMS analysis), the salt prodrug presents in equilibrium with its acid form. This is the reason for the appearance of adducts of the acid form.

FT-IR characterization of proD2 **(Figure 4.6.b)** produced a new absorption band at 1722 cm^{-1}, which represents the ester carbonyl stretch. Also the carboxylate carbonyl absorption band at 1556 cm^{-1} was intensified compared to the parent drug. It is noticed that the band of the OH bonds is missing in the spectrum of proD2, which indicates that the OH of the attached linker are ionized in the form of sodium salt. ProD2 was detected by UPLC at a retention time of 1.45 minutes **(Figure 4.6.c)**.

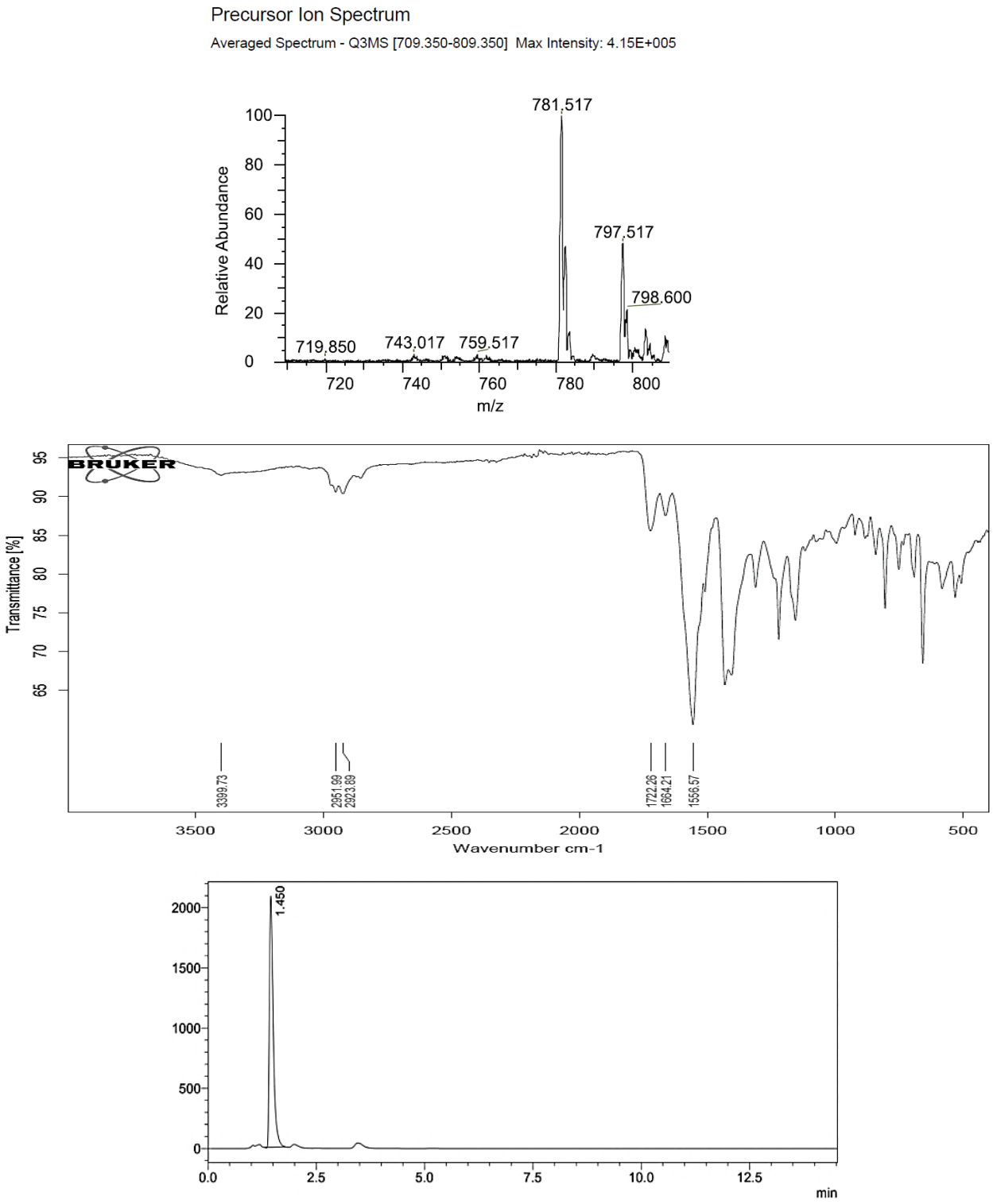

Figure 4. 6: Chemical characterization of proD2. +ESI-MS analysis (a), FT-IR spectrum (b), and UPLC detection (c) of proD2.

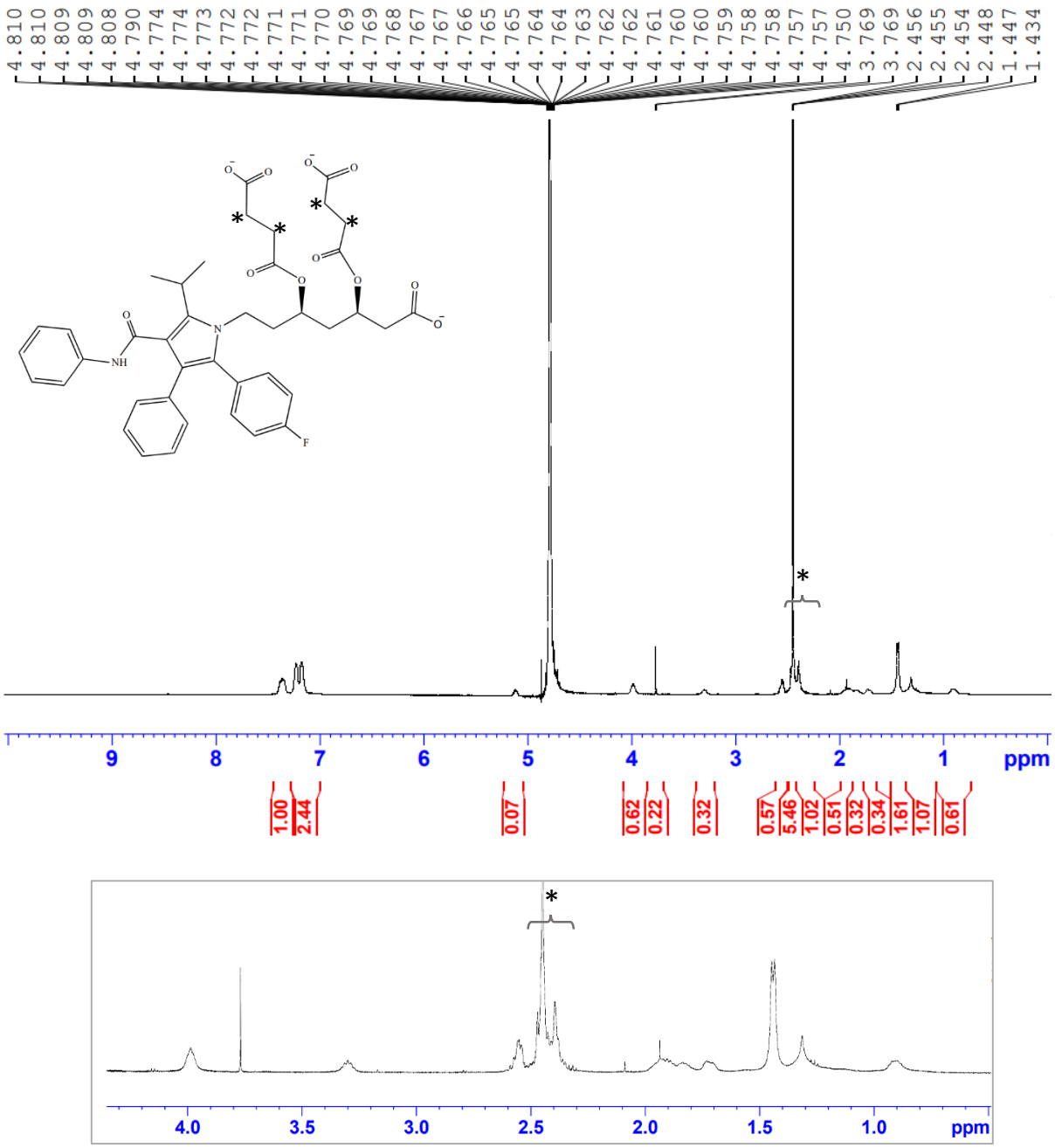

Figure 4. 7:^{1}H-NMR spectrum of proD2 in D_2O. The protons of the succinic linkers can be identified at 2.3-2.5 ppm.

4.5.Characterization of ProD3

ProD3: ^{1}H-NMR (400 MHz, D_2O) δ ppm: 1.34-1.4 (dd, 6H, C<u>H</u>$_3$-CH), 1.94-2.05 (m, 2H, CH-C<u>H</u>$_2$-CH), 2.1 (m, 2H, CH$_2$-C<u>H</u>$_2$-CH), 2.2 (m, 2H, CH-C<u>H</u>$_2$-C=O), 2.5 (m, 1H, (CH$_2$)$_2$-C<u>H</u>-O), 2.7 (m, 1H, (CH$_2$)$_2$-C<u>H</u>-O), 3.3 (m, 1H, (CH$_3$)$_2$-C<u>H</u>-Ar), 3.77 (s, 1H, N<u>H</u>), 4.09 (t, 2H, CH$_2$-C<u>H</u>$_2$-N), 6.90-6.94 (t, 2H, Aromatic H), 7 (d, 2H, Aromatic H), 7.14-7.25 (m, 7H, Aromatic H), 7.36-7.50 (m, 8H, Aromatic H), 7.54-7.64 (m, 3H, Aromatic H). **(Figure 4.10)**.

^{1}H-NMR confirmed the successful synthesis of proD3. Signals between 6.9-7.6 ppm confirmed the presence of extra eight protons in the aromatic region of the spectrum, which corresponds to the protons of the phthalic linkers. LC-MS analysis of atorvastatin proD3 **(Figure 4.9.a)** generated a signal for the salt form at 877.4 m/z. Signals at 899.5 and 915.4 m/z indicated the presence of Na and K adducts. The signal at 893.3 m/z most likely represents the K adduct of the acid form of the prodrug.

In the FT-IR spectrum of proD3 **(Figure 4.9.b)**, a new band for the ester carbonyl appeared at 1711 cm^{-1} .The absorption at the carboxylate carbonyl stretch (1562 cm^{-1}) was noticeably increased compared with the parent drug, as the structure of proD3 contains extra carbonyl bonds. No OH band is visible, because the acid OH groups of the linker moieties were in the salt form.

ProD3 was detected by UPLC at 2.0 minutes. A minor product (5%) was noticed by UPLC analysis **(Figure 4.9.c)**. The other product is expected to be the mono-esterified form of the prodrug, and it was detected by UPLC as a small split peak because it is a mixture of two structures. **Figure 4.8** illustrates the structures of the mono-esterified proD3.

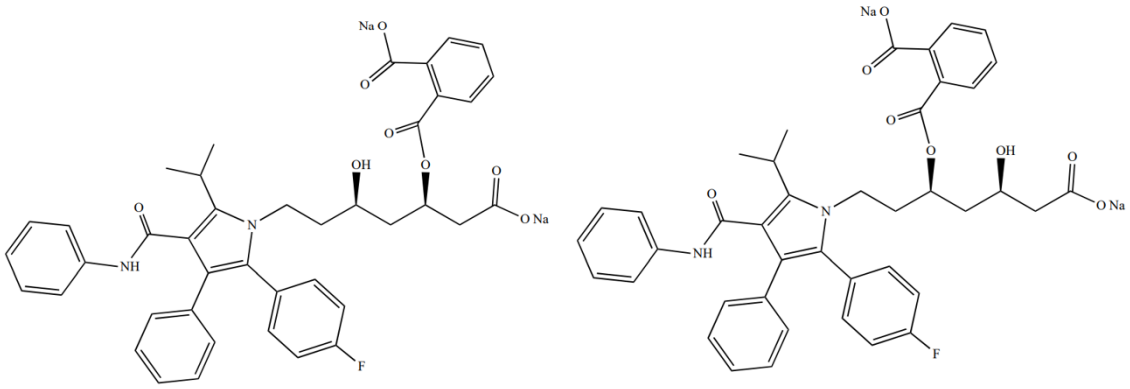

Figure 4. 8: Chemical structures of mono-esterified proD3.

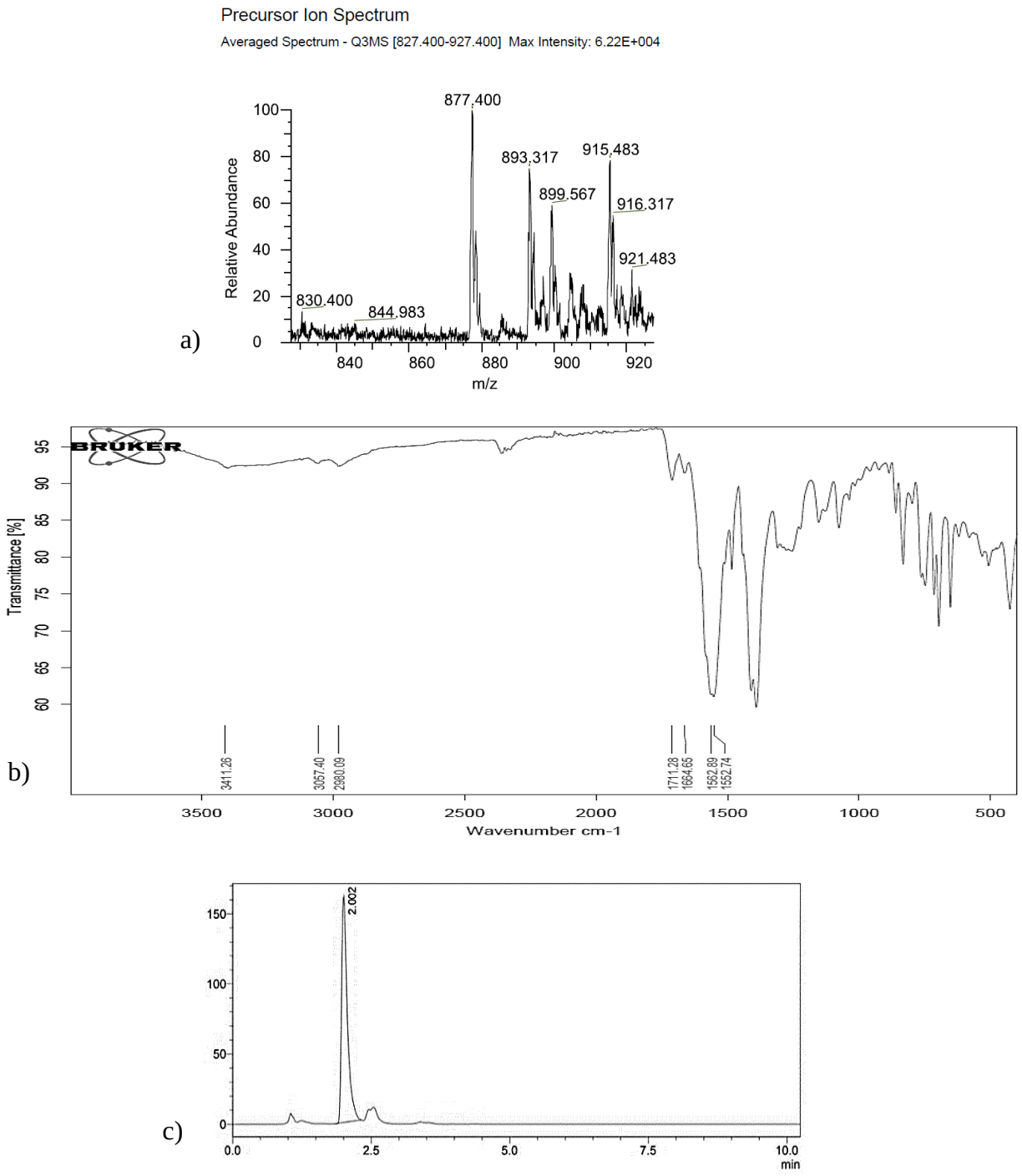

Figure 4. 9: Chemical characterization of proD3. +ESI-MS analysis (a), FT-IR spectrum (b), and UPLC detection (c) of proD3.

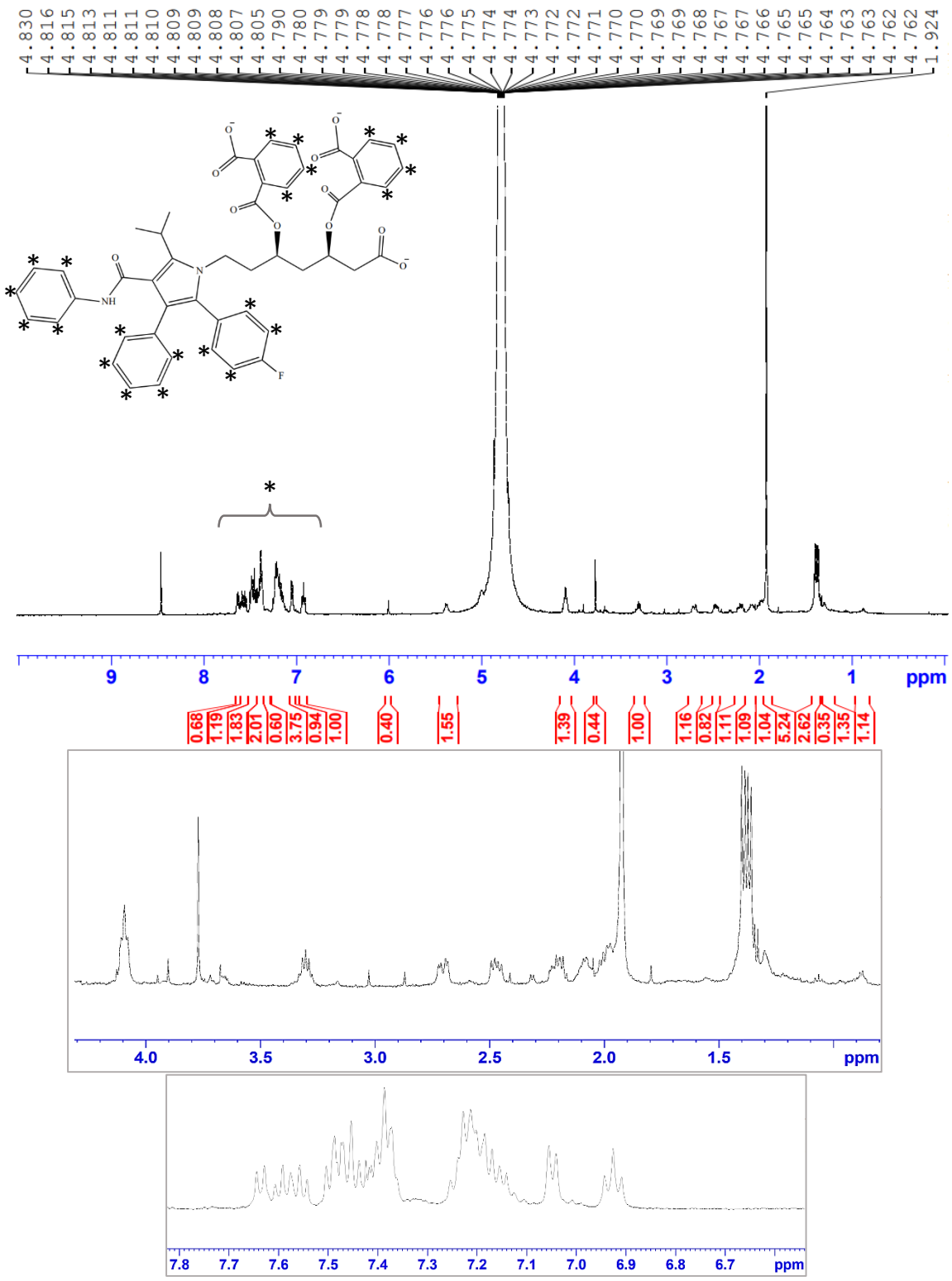

Figure 4. 10:^{1}H-NMR spectrum of proD3 in D_2O. The protons of the phthalic linkers were identified as additional signals in the aromatic region of the spectrum.

4.6. *In vitro* intraconversion of atorvastatin prodrugs

The three synthesized atorvastatin prodrugs were subjected to *in vitro* hydrolysis testing, to study the kinetics of prodrugs intraconversion to the parent drug (atorvastatin). The prodrugs convert to the parent drug by intramolecular ester hydrolysis that occurs by a nucleophilic attack of the carboxyl anion at the carbonyl of the ester. This reaction leads to the cyclization of the linker and liberation of the parent drug **(Scheme 3)**.

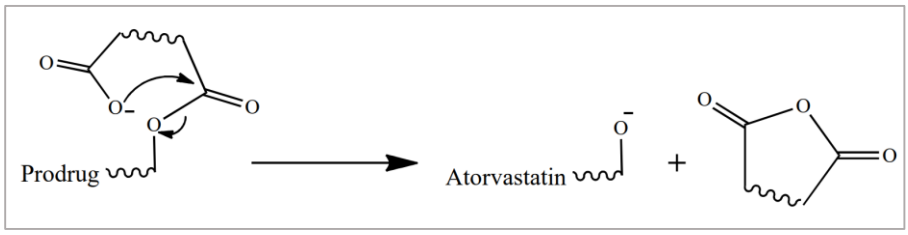

Scheme 3: Mechanism of prodrug intramolecular hydrolysis and parent drug release.

Prodrug hydrolysis was tested at a constant temperature of 37 ℃ to demonstrate prodrug behavior in the human body. Hydrolysis media of 0.1N acid, pH of 3, pH of 6.8, and blood plasma were used to channel the pH variation that drugs encounter during their journey along the gastrointestinal tract to blood. The rate of conversion (k_{obs}) was extrapolated from a plot of the prodrug concentration vs. time, and the value of k_{obs} was used to calculate the half-life ($t_{1/2}$) of prodrug conversion.

UPLC monitoring of prodrugs hydrolysis showed that an intermediate was being produced before the appearance of the parent drug. The intermediate is most probably the mono-esterified form of the prodrug. There are two forms of the mono-esterified prodrug, with the linker attached either to the β or δ hydroxyl group.

ProD1 was hydrolyzed in acidic media following a first order kinetics; and eventually, the prodrug and the intermediates were completely converted to the parent drug. While in pH of 6.8, the hydrolysis was much slower and even incomplete after the passage of one month.

The half-lives of hydrolysis of proD1 in 0.1 N HCl solution, pH of 3, and pH of 6.8 were 102 hours,161 hours, and 693 hours, respectively **(Figure 4.12.b, 4.14.b,** and **4.16.b)**. The reaction was faster in more acidic media because the cyclization of the anhydride linker, and hence the hydrolysis of the prodrug, was being acid catalyzed. ProD1 exhibited complete, first order hydrolysis in blood plasma. The half-life of the hydrolysis was 198 hours **(Figure 4.18.b)**. Prodrug hydrolysis in plasma was faster than the hydrolysis in pH 6.8 buffer, this suggests that at this point, the reaction may occur as base catalyzed ester hydrolysis.

The UPLC spectra of analysis at the beginning and ending of the kinetic study of proD1 in each medium are shown in **Figures 4.11, 4.13, 4.15,** and **4.17**. The disappearance of proD1 as detected by UPLC, along with the appearance of the intermediates and the parent drug in each medium are plotted in reference to time in **Figures 4.12.a, 4.14.a, 4.16.a,** and **4.18.a.**

ProD2 exhibited complete conversion to the parent drug in pH 3 buffer **(Figure 4.19)**. The half-life of conversion was 216 hours **(Figure 4.20)**. On the other hand, proD2 was stable in pH 6.8 buffer and plasma, and no hydrolysis was noticed in either medium **(Figure 4.21)**. ProD2 was completely insoluble in 0.1N acid solution, so the conversion in this medium was unable to be detected. The same happened with proD3 in both 0.1N acid solution and buffer of pH 3. And similar to proD2, proD3 showed no hydrolysis in pH 6.8 and plasma **(Figure 4.22)**.

It was found that the hydrolysis of proD1 was faster than that of proD2 in pH 3. Moreover, proD2 did not exert conversion in pH 6.8 and plasma, unlike proD1. This is owed to the difference in the

linker attached to each prodrug. The maleate linker (proD1) has a carbon-carbon double bond within its structure, which helps in restricting the prodrug in a conformation that has more proximity of the reacting centers, and creates a strain effect that is relieved by forming a tetrahedral intermediate followed by cyclization of the linker and release of the parent drug. The succinic linker of proD2 lacks that double bond and it mainly exists in an extended conformation in which the reactive centers are distant, this prodrug system requires higher activation energy for the prodrug to reach the tetrahedral intermediate and intraconvert. Also, the stability of proD3 indicates that the prodrug system does not exist in a favorable orientation for the nucleophilic attack to occur.

The results of the hydrolysis and/or stability of the three prodrugs were compatible with the hypothesis of Bruice and Karaman, the intraconversion was dependent on the structural features of the attached linker; and the higher the strain energy, the lower activation energy required for the intramolecular reaction. ProD1 has the maleate linker and exerted full hydrolysis which was catalyzed by the strain imparted by the double bond of maleic anhydride. The presence of a double bond in the structure of the linker increases the strain energy of the prodrug system, which requires (relatively) low activation energy for the cyclization of the linker into an anhydride and at the same time the release of the parent drug. This is unlike proD2 with the succinate linker which has lower strain energy and requires higher activation energy for the intramolecular reaction to occur. Even though proD2 has a very similar structure to proD1, the absence of the double bond in the structure of the succinate linker lowers the strain energy in this prodrug, because the single bonds and what accompanies them of flexibility makes the linker exist mainly in an extended conformation which is not strained enough to allow cyclization. Despite this, proD2 exerted full hydrolysis in pH 3, this is because Bruice's dicarboxylic intramolecular hydrolysis is an acid catalyzed reaction, and

in highly acidic medium, acid catalysis lowers the activation energy for the intramolecular reaction. At higher pH values the acid catalysis was missing, so the conversion reaction did not seem to be occurring. Although, the conversion might actually be happening in an extremely low rate that is almost undetectable. ProD3 has the phthalate linker. The phthalate linker has an aromatic ring and when linked to the parent drug, it was expected to be highly strained and exert catalyzed intaconversion. As this prodrug was insoluble in low pH, the acid catalysis of the intraconversion could not be detected, but the experimental results showed that the prodrug was stable in pH 6.8 and in plasma (pH 7.4), this indicates that the prodrug was restricted to an unfavorable conformation for ester hydrolysis, which might be owed to adverse geometrical factors (the distance between the two reactive centers and the angle of attack).

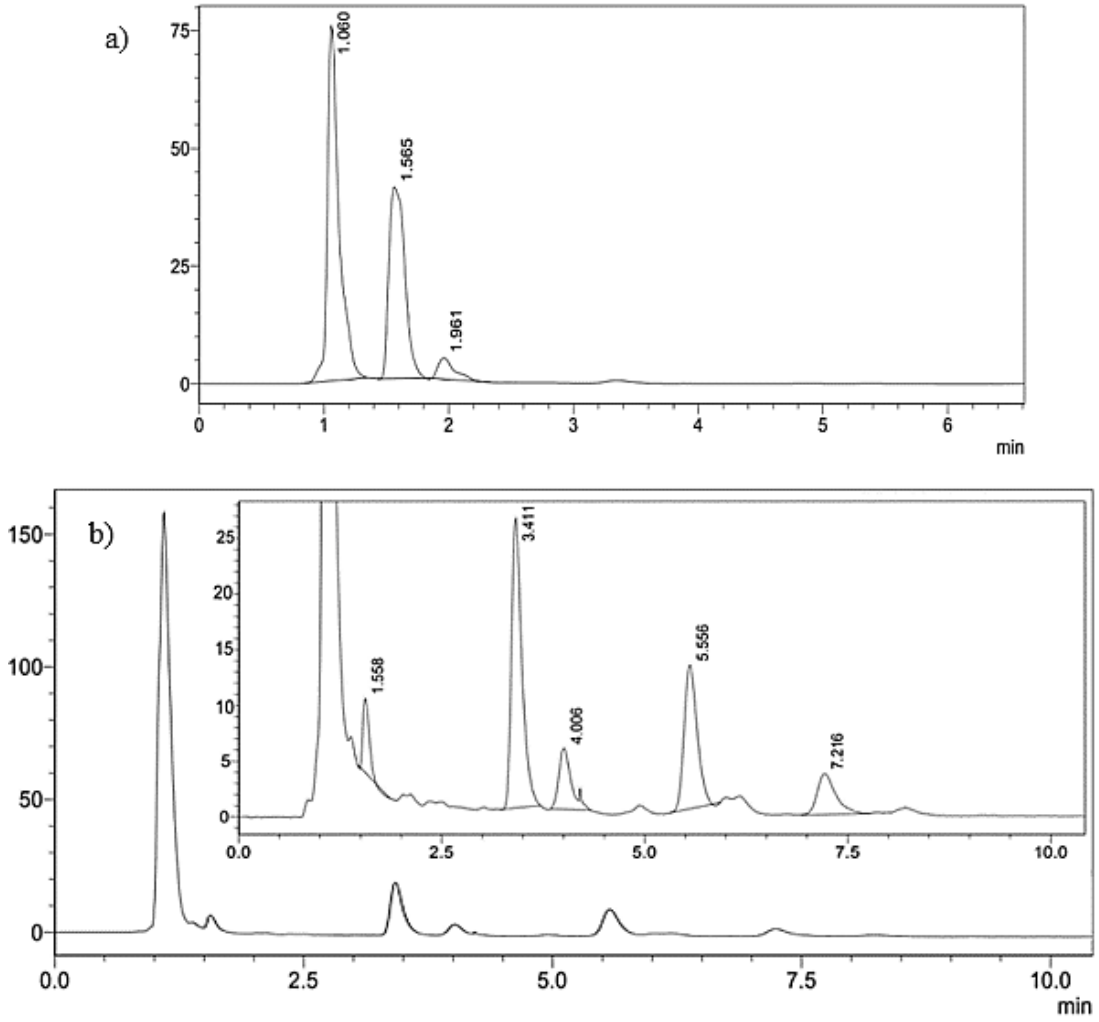

Retention time (min)	Name of peak
1.06	Maleic acid
1.5	proD1
1.9	Intermediate
3.4	Atorvastatin (ionized)
5.5	Atorvastatin acid
7.2	Atorvastatin lactone

Figure 4. 11: *In vitro* intraconversion of proD1 in 0.1N HCl solution after 3 hours (a), and after 270 hours (b) of incubation in 0.1N acid solution.

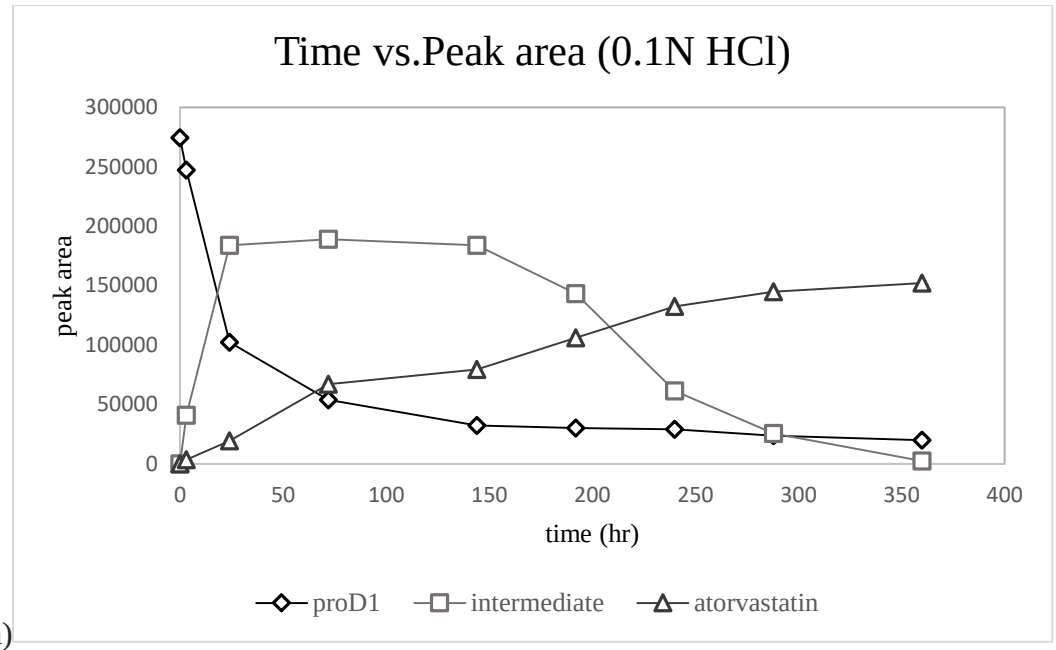

a)

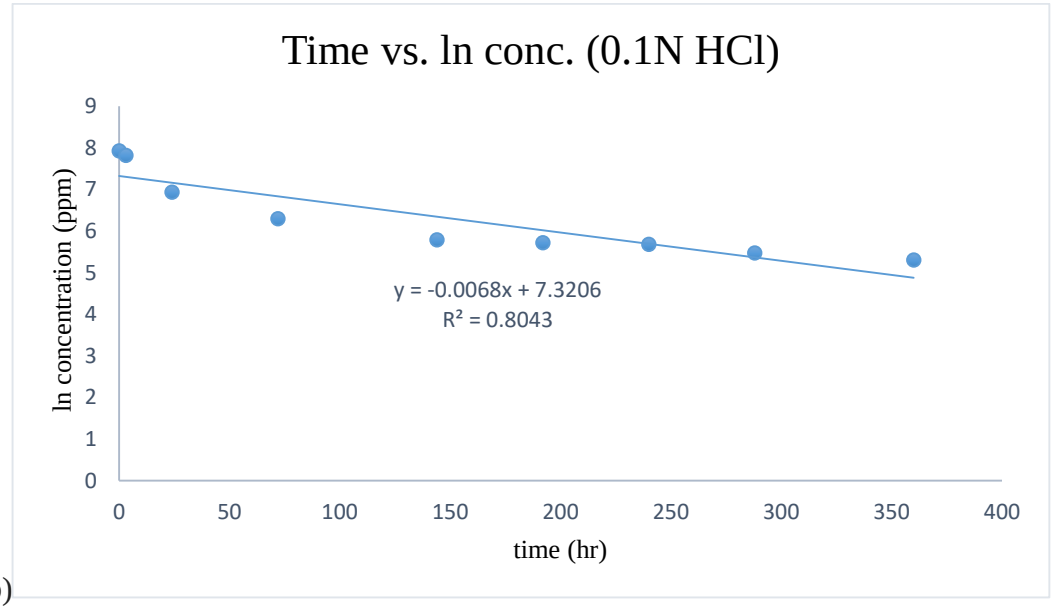

b)

Figure 4. 12 (a): proD1 hydrolysis, intermediate appearance and atorvastatin release in 0.1N HCl. (b): First-order hydrolysis plot of proD1 in 0.1N HCl, k_{obs} = 6.8× 10^{-3} hr^{-1}.

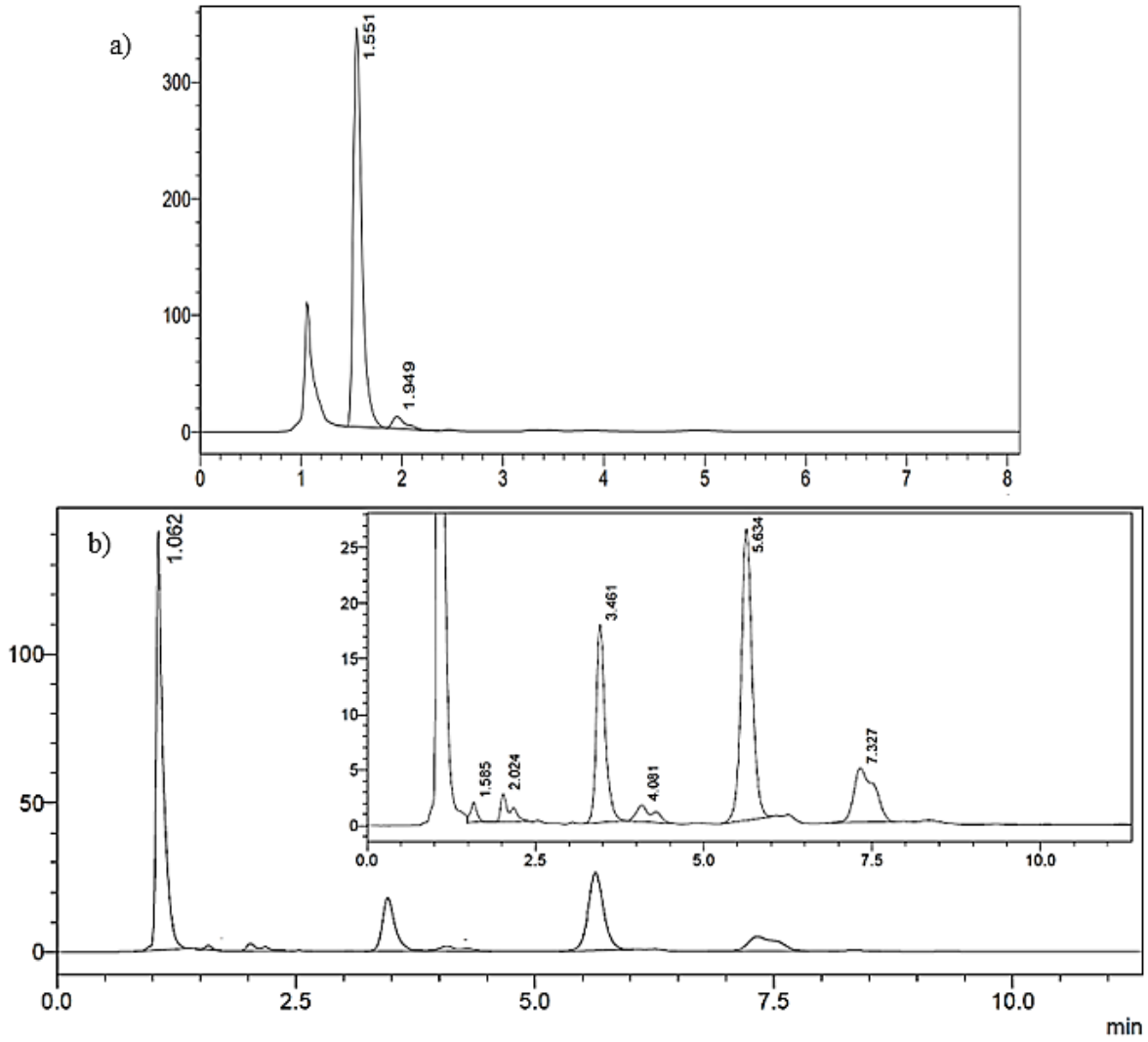

Retention time (min)	Name of peak
1.06	Maleic acid
1.5	proD1
1.9	Intermediate
3.4	Atorvastatin (ionized)
5.	Atorvastatin acid
7.3	Atorvastatin lactone

Figure 4. 13: *In vitro* intraconversion of proD1 in pH 3 after 3 hours (a) and after 288 hours (b) of incubation in pH 3 buffer.

a)

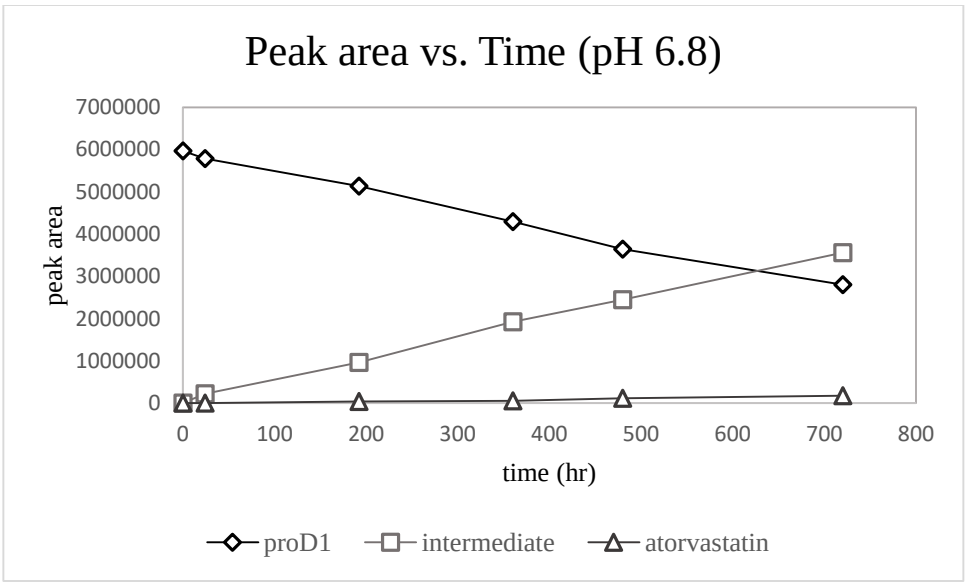

b)

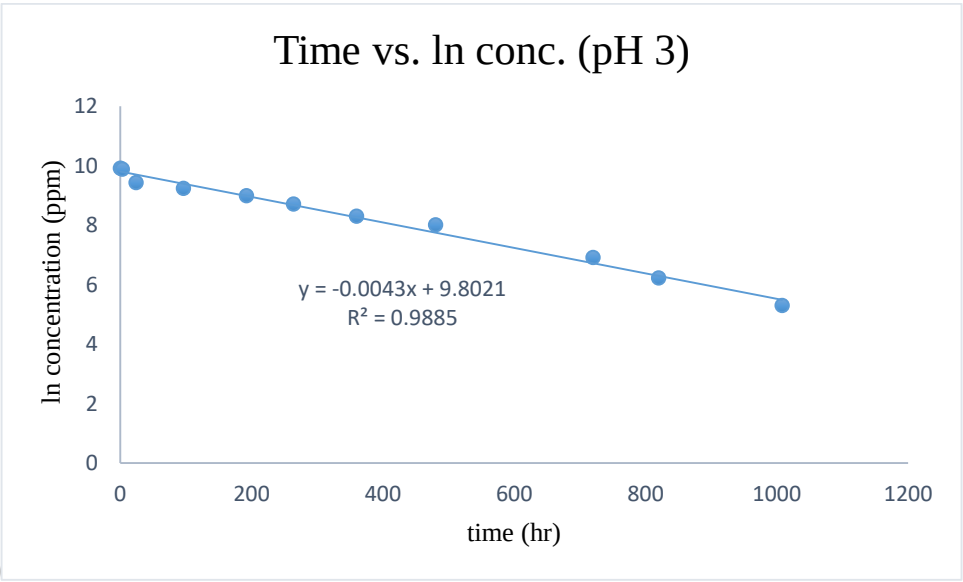

Figure 4. 14 (a): proD1 hydrolysis, intermediate appearance and atorvastatin release in pH3 buffer.
(b): First-order hydrolysis plot of proD1 in pH3 buffer, , k_{obs} = 4.3× 10^{-3} hr^{-1}.

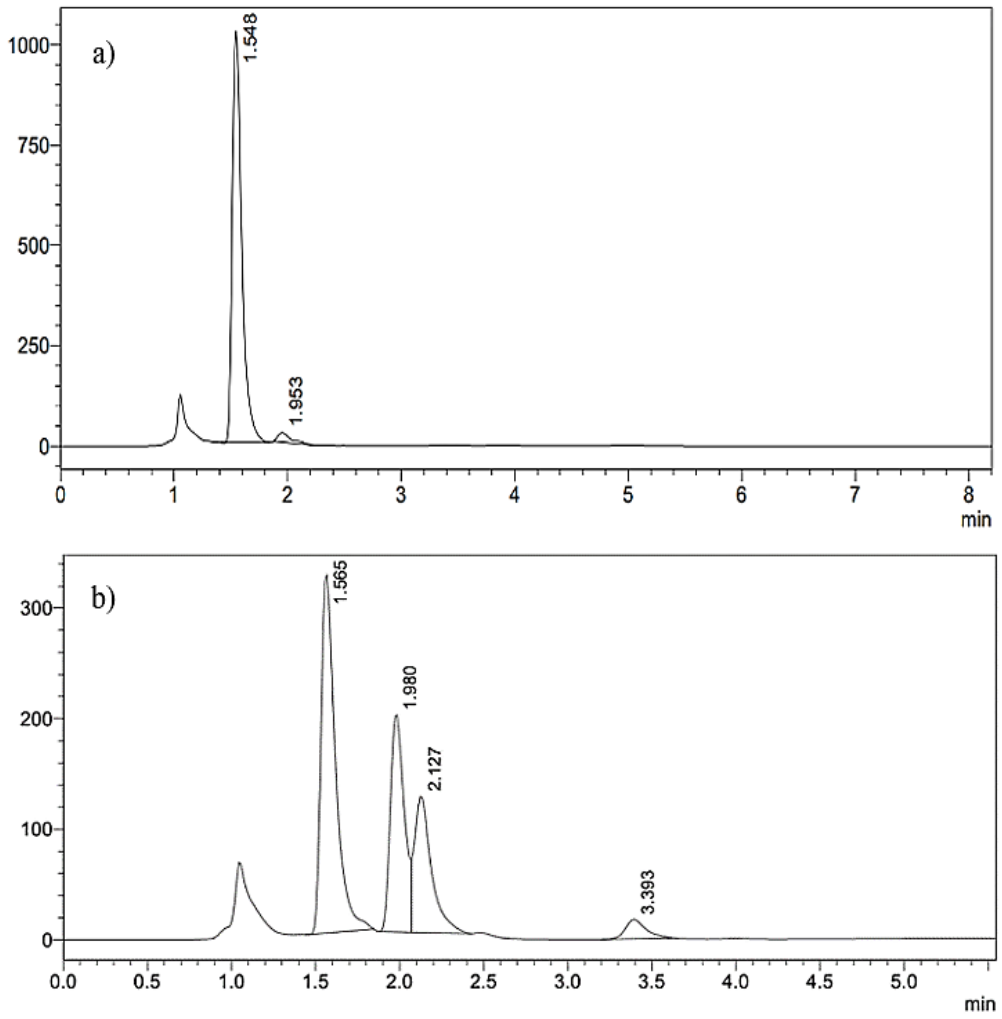

Figure 4. 15: *In vitro* intraconversion of proD1 in pH 6.8 after 24 hours (a) and after 720 hours (b) of incubation in pH 6.8 buffer. The peaks detected at 1.06 min, 1.5 min, and 3.39 min represent maleic acid, proD1, and atorvastatin, respectively. The two peaks at 1.9 min and 2.1 min represent the two forms of the mono-esterified prodrug (intermediates).

a)

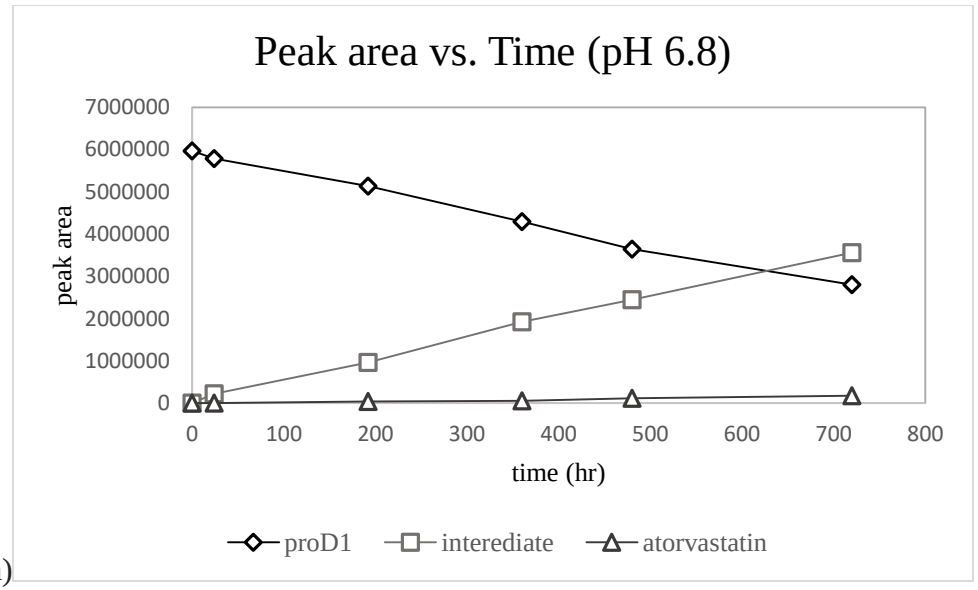

b)

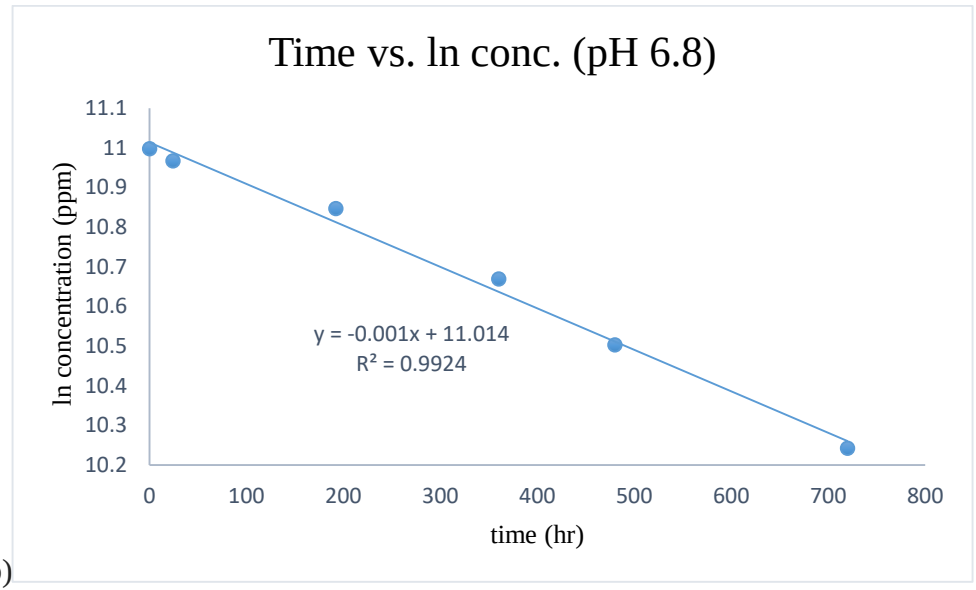

Figure 4. 16 (a): ProD1 hydrolysis, intermediate appearance and atorvastatin release in pH 6.8 buffer. (b): First-order hydrolysis plot of proD1 in pH 6.8 buffer, , $k_{obs} = 1 \times 10^{-3} hr^{-1}$.

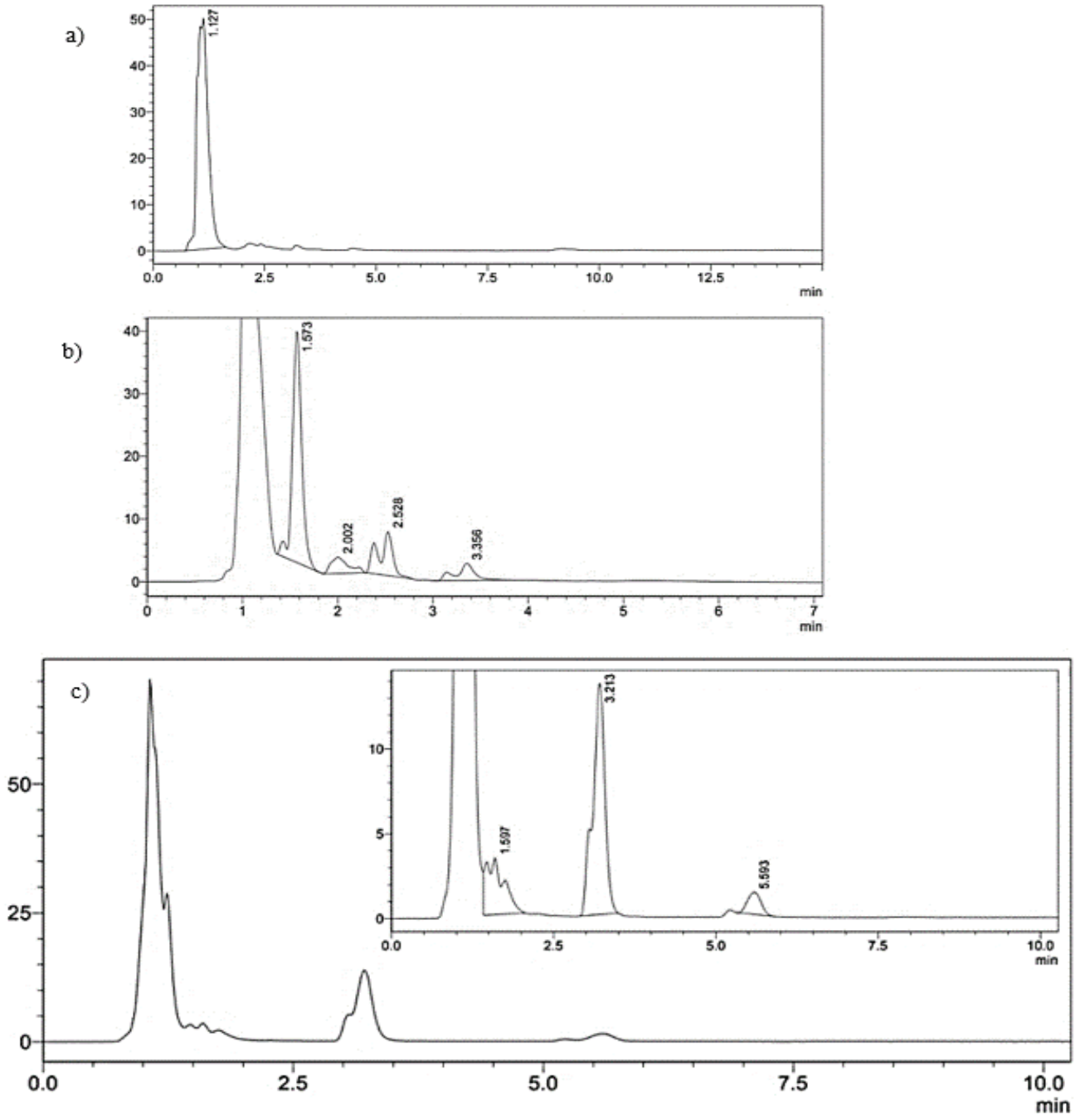

Figure 4. 17 (a): UPLC spectrum of blank plasma. (b): *In vitro* intraconversion of proD1 in human plasma after 24 hours. The peak at 1.5 min represents proD1, the peaks detected at 2.0-2.5 min represent the intermediates of the hydrolysis,and the peak at 3.3 min is for atorvastain. (c): *In vitro* intraconversion of proD1 in human plasma after 336 hours. The peaks at 3.2 and 5.5 min represent two forms of atorvastatin.

a)

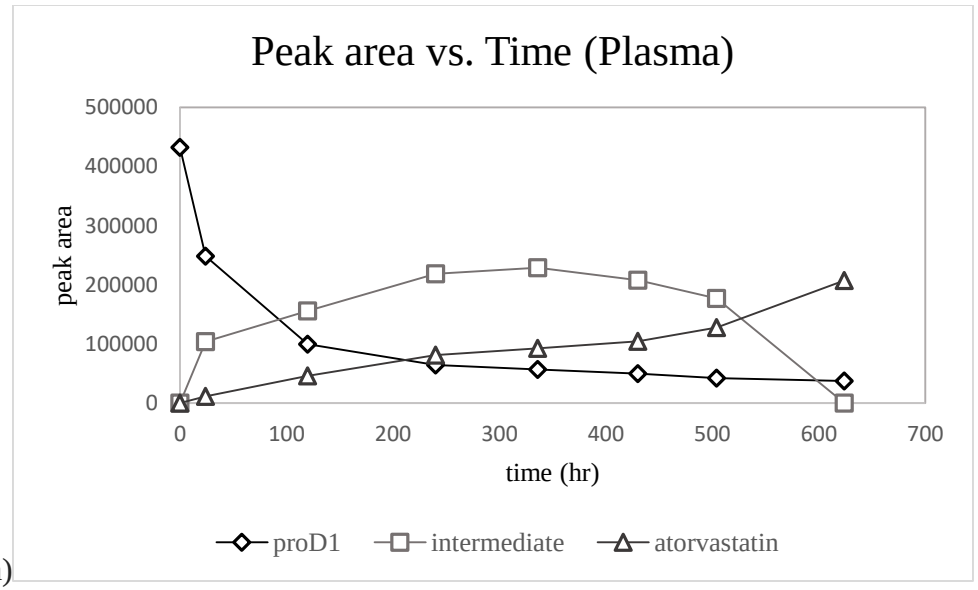

b)

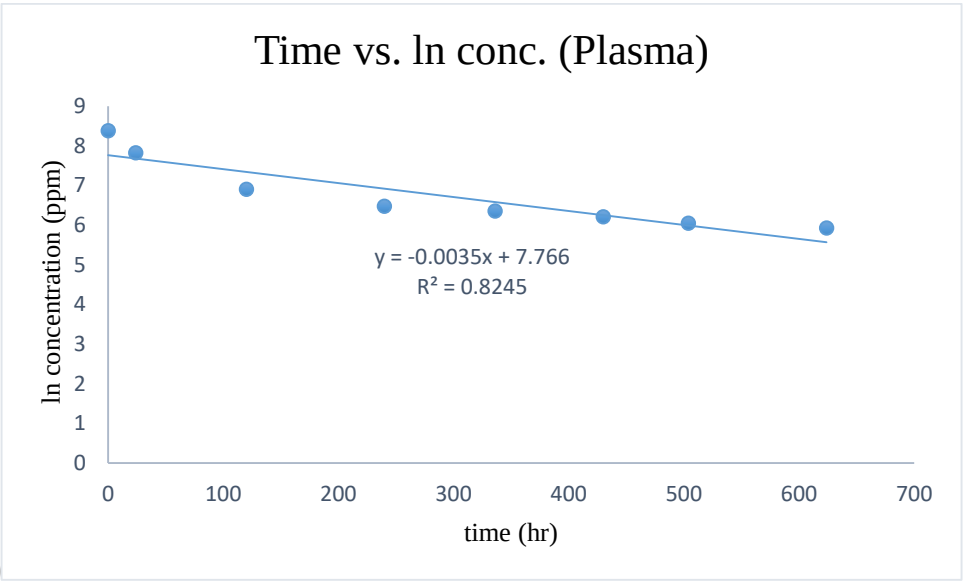

Figure 4. 18 (a): proD1 hydrolysis, intermediate appearance and atorvastatin release in human plasma. (b): First-order hydrolysis plot of proD1 in human plasma, , $k_{obs} = 3.5 \times 10^{-3}$hr^{-1}.

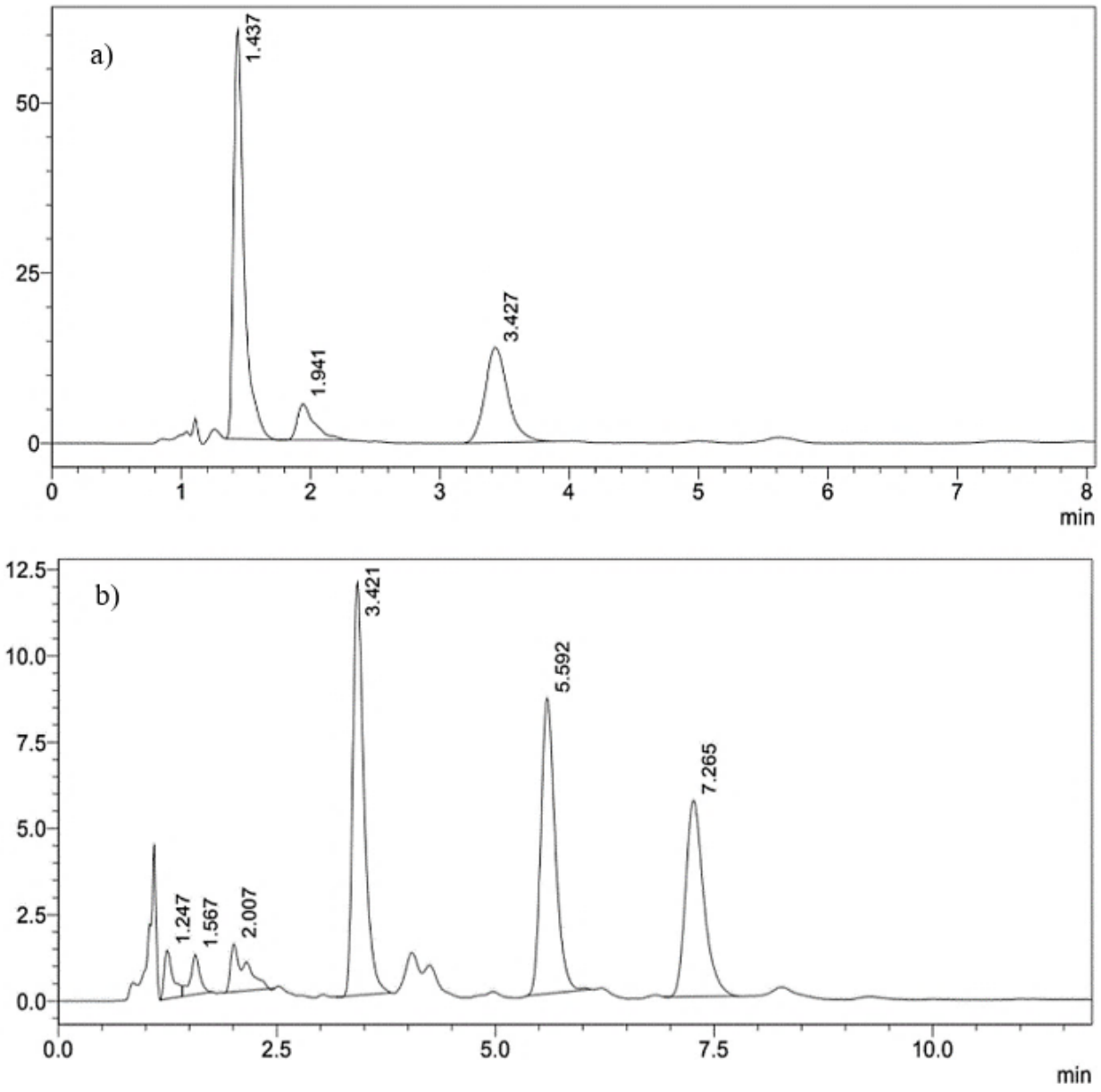

Figure 4. 19: *In vitro* intraconversion of proD2 in 0.1N HCl solution after 5 hours (a), and after 450 hours (b) of incubation in 0.1N acid solution. The peak at 1.4 min (a) represents proD2, the peaks detected at 3.4, 5.5, and 7.2 min (b) represent the different forms of atorvastain

a)

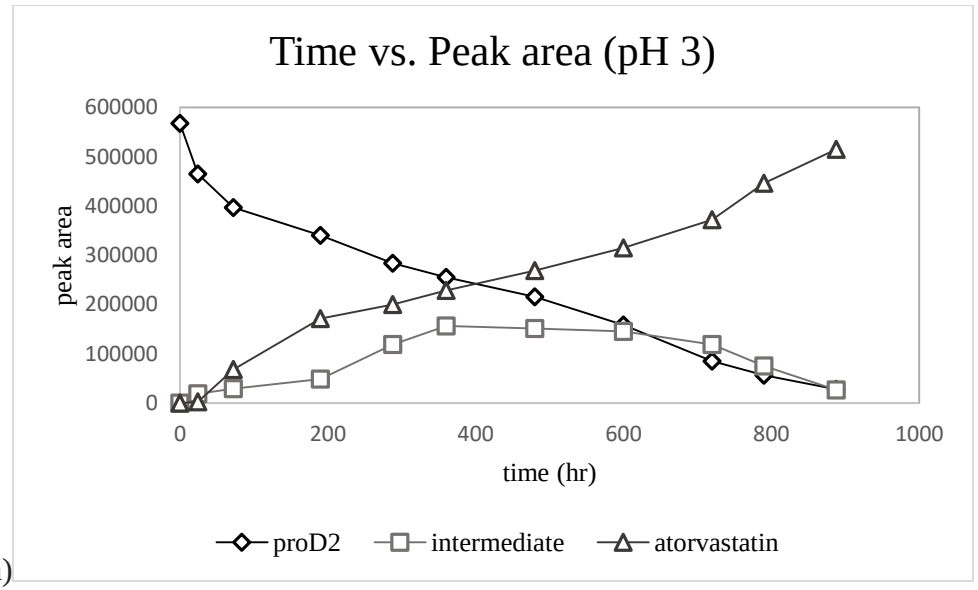

b)

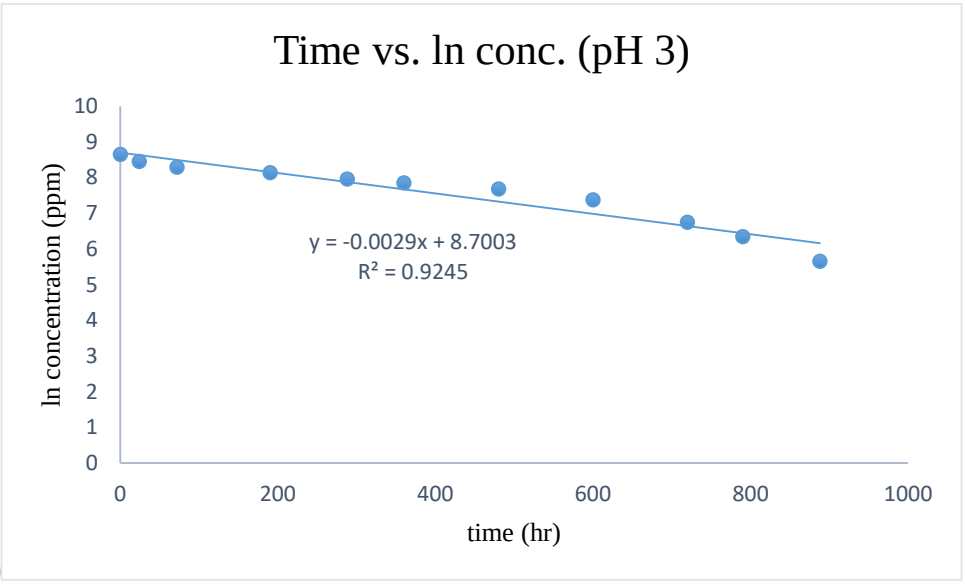

Figure 4. 20 (a): proD2 hydrolysis, intermediate appearance and atorvastatin release in 0.1N HCl. (b): First-order hydrolysis plot of proD2 in 0.1N HCl, , $k_{obs} = 2.9 \times 10^{-3}\text{hr}^{-1}$.

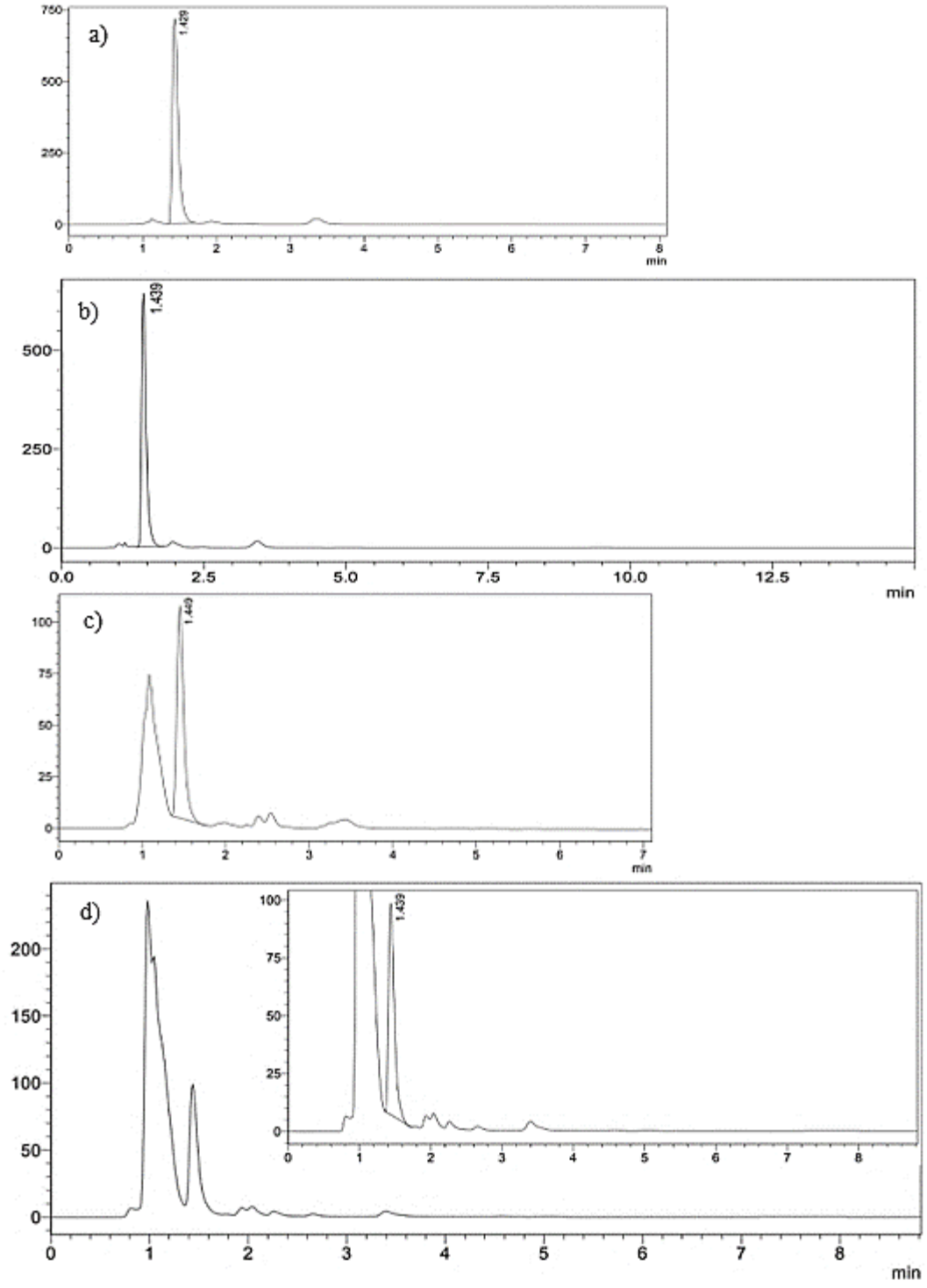

Figure 4. 21: Stability of proD2 (peak at 1.4 min) in pH 6.8 and human plasma. ProD2 spectrum after 24 hours of incubation in pH 6.8 buffer (a), and after 360 hours of incubation in pH 6.8 buffer (b). ProD2 spectrum after 24 hours of incubation in plasma (c), and after 500 hours of incubation in plasma (d).

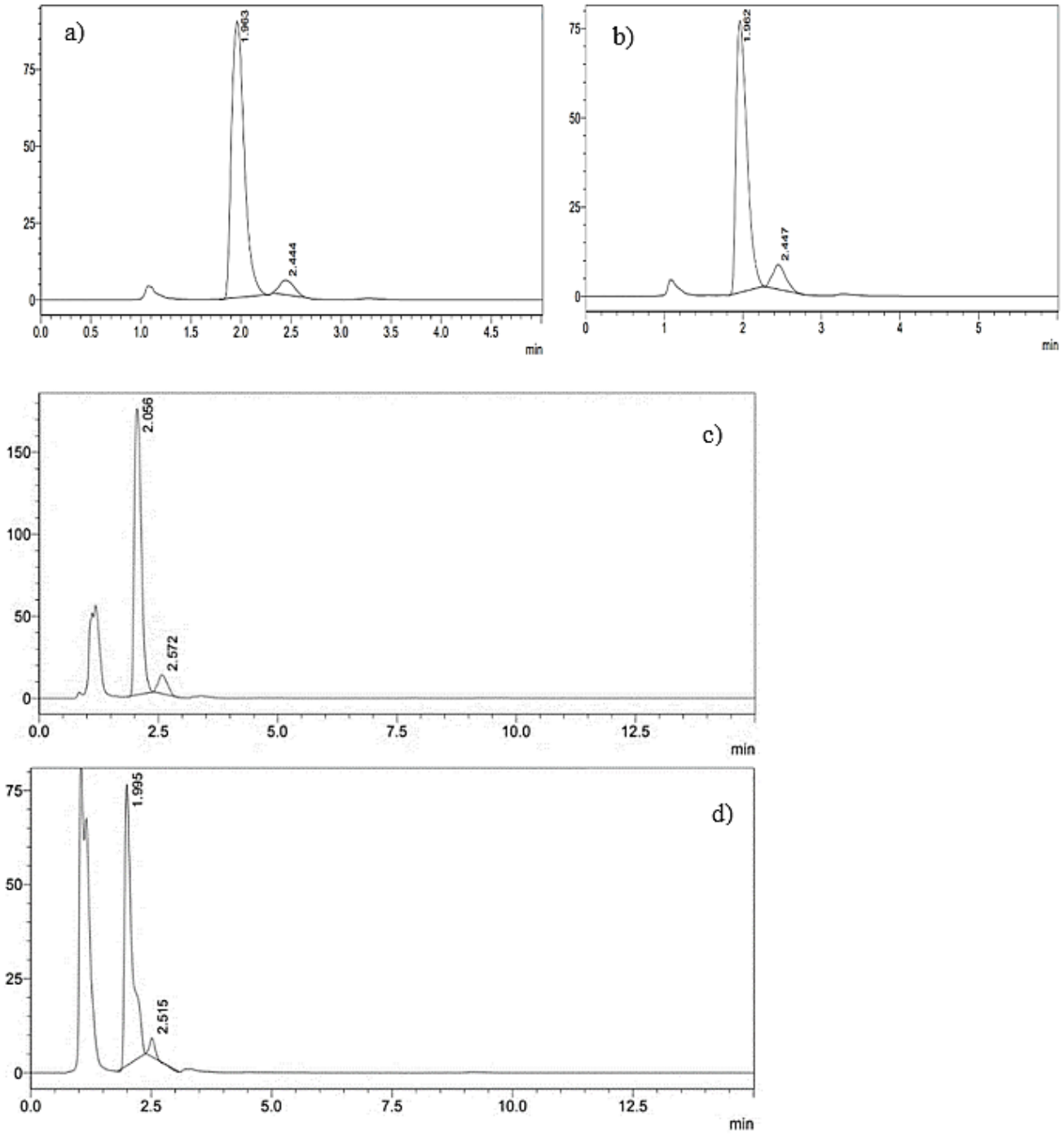

Figure 4. 22: Stability of proD3 (peak at 1.9/2.0 min) in pH 6.8 and human plasma. ProD3 spectrum after 24 hours of incubation in pH 6.8 buffer (a), and after 500 hours of incubation in pH 6.8 buffer (b). ProD3 spectrum after 24 hours of incubation in plasma (c), and after 500 hours of incubation in plasma (d).

Chapter Five

Conclusion and Future Direction

5. Conclusion and future direction

The synthesis of three new atorvastatin ester prodrugs with greater bioavailability and decreased risk of side effects is described in this thesis. Maleic anhydride, succinic anhydride, and phthalic anhydride were utilized as prodrug linkers to conceal the metabolically labile hydroxyl groups of atorvastatin, according to Bruice's enzyme model. In addition, the prodrugs showed a considerable increase in water solubility and bitter taste masking. The identity of each prodrug was confirmed using chemical characterization, melting point detection, LCMS, FT-IR, and ^{1}H-NMR analysis. Intraconversion of the prodrugs was studied *in vitro* in various pH media and blood plasma. ProD1 was able to achieve prodrug hydrolysis and parent drug release in all media. Prodrug hydrolysis half-lives were 102 hours, 161 hours, 693 hours, and 198 hours in 0.1N acid solution, pH 3 buffer, pH 6.8 buffer, and plasma, respectively. ProD2 and proD3 showed insolubility in acidic media and stability in higher pH media, with the exception of proD2 hydrolysis in pH 3 at a half-life of 216 hours.

The structural characteristics of the linker determine prodrug conversion. According to this, intramolecular hydrolysis will occur in strained prodrug complexes that are oriented in a conformation that allows the reactive sites to be close together. ProD1 was an example of this, because of the high strain energy of maleic anhydride which lowed the activation energy for the intramolecular hydrolysis. ProD1 is a good option for *in vivo* use due to its *in vitro* intrahydrolysis. ProD1 can be packaged in standard tablets, absorbed as an intact prodrug, bypass first-pass metabolism, and exert a delayed release effect due to the relatively long half-life of conversion.

In vivo studies of the kinetics of prodrug absorption and conversion should be conducted in the future. Following that, an *in vivo* evaluation of the prodrugs' efficacy in decreasing LDL-

cholesterol will be required. Furthermore, novel linkers will be tested in the synthesis of atorvastatin prodrugs, which are projected to require less energy of activation for intramolecular hydrolysis.

References

1. Simons, K. and E. Ikonen, *How cells handle cholesterol.* Science, 2000. **290**(5497): p. 1721-1726.
2. Forte, T. and A.V. Nichols, *Application of electron microscopy to the study of plasma lipoprotein structure.* Advances in lipid research, 1972. **10**: p. 1-41.
3. Gotto, A.M. and R.L. Jackson, *Structure of the plasma lipoproteins—a review.* Atherosclerosis IV, 1977: p. 177-188.
4. Craig, M. and A. Malik, *Biochemistry, cholesterol.* Treasure Island, FL: StatPearls, 2018.
5. Nichols, A.V., *Functions and interrelationships of different classes of plasma lipoproteins.* Proceedings of the National Academy of Sciences of the United States of America, 1969. **64**(3): p. 1128.
6. Dufaux, B., *Plasma lipoproteins and physical activity: a review.* Int J Sports Med, 1982; **03**: p. 123-136.
7. Eisenberg, S. and R.I. Levy, *Lipoprotein metabolism.* Advances in lipid research, 1975. **13**: p. 1-89.
8. Osborne Jr, J.C. and H.B. Brewer Jr, *The plasma lipoproteins.* Advances in protein chemistry, 1977. **31**: p. 253-337.
9. Eaton, C.B., *Hyperlipidemia.* Primary Care: Clinics in Office Practice, 2005. **32**(4): p. 1027-1055.
10. Sevanian, A., L. Asatryan, and O. Ziouzenkova, *Low density lipoprotein (LDL) modification: basic concepts and relationship to atherosclerosis.* Blood purification, 1999. **17**(2-3): p. 66-78.
11. Michael, S. and L. Goldstein, *A receptor-mediated pathway for cholesterol homeostasis.* Physiology Or Medicine: 1981-1990, 1993: p. 284.
12. Virani, S.S., *et al*., *Heart disease and stroke statistics—2020 update: a report from the American Heart Association.* Circulation, 2020. **141**(9): p. e139-e596.
13. Nelson, R.H., *Hyperlipidemia as a risk factor for cardiovascular disease.* Primary Care: Clinics in Office Practice, 2013. **40**(1): p. 195-211.

14. Ross, R. and L. Harker, *Hyperlipidemia and atherosclerosis.* Science, 1976. **193**(4258): p. 1094-1100.

15. Tabas, I., G. García-Cardeña, and G.K. Owens, *Recent insights into the cellular biology of atherosclerosis.* Journal of Cell Biology, 2015. **209**(1): p. 13-22.

16. Cooney, M., *et al*., *HDL cholesterol protects against cardiovascular disease in both genders, at all ages and at all levels of risk.* Atherosclerosis, 2009. **206**(2): p. 611-616.

17. Stone, N.J., *et al*., *2013 ACC/AHA guideline on the treatment of blood cholesterol to reduce atherosclerotic cardiovascular risk in adults: a report of the American College of Cardiology/American Heart Association Task Force on Practice Guidelines.* Journal of the American College of Cardiology, 2014. **63**(25 Part B): p. 2889-2934.

18. Martinez-Hervas, S. and J.F. Ascaso, *Hypercholesterolemia.* Encyclopedia of Endocrine Diseases-Elsevier, 2018. **01**: p. 1-7.

19. Goldstein, J.L., *Familial hypercholesterolemia.* Medical Grand Rounds-Parkland Memorial Hospital, 1974.

20. Ramasamy, I., *Update on the molecular biology of dyslipidemias.* Clinica chimica acta, 2016. **454**: p. 143-185.

21. Schachter, M., *Chemical, pharmacokinetic and pharmacodynamic properties of statins: an update.* Fundam Clin Pharmacol, 2005. **19**(1): p. 117-25.

22. Jacobson, T.A., *et al*., *National lipid association recommendations for patient-centered management of dyslipidemia: part 1—full report.* Journal of clinical lipidology, 2015. **9**(2): p. 129-169.

23. Group, H.P.S.C., *Randomized trial of the effects of cholesterol-lowering with simvastatin on peripheral vascular and other major vascular outcomes in 20,536 people with peripheral arterial disease and other high-risk conditions.* Journal of vascular surgery, 2007. **45**(4): p. 645-654. e1.

24. Sever, P.S., *et al*., *Prevention of coronary and stroke events with atorvastatin in hypertensive patients who have average or lower-than-average cholesterol concentrations, in the Anglo-Scandinavian Cardiac Outcomes Trial—Lipid Lowering Arm (ASCOT-LLA): a multicentre randomised controlled trial.* The Lancet, 2003. **361**(9364): p. 1149-1158.

25. Sacks, F.M., *et al*., *The effect of pravastatin on coronary events after myocardial infarction in patients with average cholesterol levels.* New England Journal of Medicine, 1996. **335**(14): p. 1001-1009.

26. *Lipitor [package insert]. New York, NY: Parke-Davis-Pfizer, Inc; 2019.*

27. *Lescol/Lescol XL [package insert]. East Hanover, NJ: Novartis Pharmaceuticals Corporation; 2012.*

28. *Mevacor [package insert]. Morgantown, WV: Mylan Pharmaceuticals, Inc; 2014.*

29. *Pravachol [package insert]. Princeton, NJ: Bristol-Myers Squibb Company; 2016.*

30. *Zocor [package insert]. Whitehouse Station, NJ: Merck & Co, Inc; 2015.*

31. *Livalo [package insert]. Montgomery, AL: Kowa Pharmaceuticals America, Inc; 2016.*

32. *Crestor [package insert]. Wilmington, DE: AstraZeneca Pharmaceuticals, LP; 2016.*

33. Jones, P., S. Kafonek, and D. Hunninghake, *Comparative dose efficacy study of atorvastatin versus simvastatin, pravastatin, lovastatin, and fluvastatin in patients with hypercholesterolemia (the CURVES study).* The American journal of cardiology, 1998. **81**(5): p. 582-587.

34. Jones, P.H., *et al*., *Comparison of the efficacy and safety of rosuvastatin versus atorvastatin, simvastatin, and pravastatin across doses (STELLAR Trial).* The American journal of cardiology, 2003. **92**(2): p. 152-160.

35. Saito, Y., *et al*., *A randomized, double-blind trial comparing the efficacy and safety of pitavastatin versus pravastatin in patients with primary hypercholesterolemia.* Atherosclerosis, 2002. **162**(2): p. 373-379.

36. Karr, S., *Epidemiology and management of hyperlipidemia.* The American journal of managed care, 2017. **23**(9 Suppl): p. S139-S148.

37. Joy, T.R. and R.A. Hegele, *Narrative review: statin-related myopathy.* Annals of internal medicine, 2009. **150**(12): p. 858-868.

38. Last, A.R., J.D. Ference, and E.R. Menzel, *Hyperlipidemia: drugs for cardiovascular risk reduction in adults.* American family physician, 2017. **95**(2): p. 78-87.

39. Einarsson, K., *et al*., *Bile acid sequestrants: mechanisms of action on bile acid and cholesterol metabolism.* European journal of clinical pharmacology, 1991. **40**(1): p. S53-S58.

40. Knapp, H.H., *et al*., *Efficacy and safety of combination simvastatin and colesevelam in patients with primary hypercholesterolemia.* The American journal of medicine, 2001. **110**(5): p. 352-360.

41. *Zetia [package insert]. Whitehouse Station, NJ: Merck & Co, Inc; 2013.*

42. McKenney, J., *et al*., *LDL-C goal attainment with ezetimibe plus simvastatin coadministration vs atorvastatin or simvastatin monotherapy in patients at high risk of CHD.* Medscape General Medicine, 2005. **7**(3): p. 3.

43. Ballantyne, C.M., *et al*., *Effect of ezetimibe coadministered with atorvastatin in 628 patients with primary hypercholesterolemia: a prospective, randomized, double-blind trial.* Circulation, 2003. **107**(19): p. 2409-2415.

44. Brown, W., *et al*., *Effects of fenofibrate on plasma lipids. Double-blind, multicenter study in patients with type IIA or IIB hyperlipidemia.* Arteriosclerosis: An Official Journal of the American Heart Association, Inc., 1986. **6**(6): p. 670-678.

45. Insua, A., *et al*., *Fenofibrate or gemfibrozil for treatment of types IIa and IIb primary hyperlipoproteinemia: a randomized, double-blind, crossover study.* Endocrine Practice, 2002. **8**(2): p. 96-101.

46. Enger, C., *et al*., *Pharmacoepidemiology safety study of fibrate and statin concomitant therapy.* The American journal of cardiology, 2010. **106**(11): p. 1594-1601.

47. Probstfield, J.L. and D.B. Hunninghake, *Nicotinic acid as a lipoprotein-altering agent: therapy directed by the primary physician.* Archives of internal medicine, 1994. **154**(14): p. 1557-1559.

48. Investigators, A.-H., *Niacin in patients with low HDL cholesterol levels receiving intensive statin therapy.* New England Journal of Medicine, 2011. **365**(24): p. 2255-2267.

49. Navarese, E.P., *et al*., *Effects of proprotein convertase subtilisin/kexin type 9 antibodies in adults with hypercholesterolemia: a systematic review and meta-analysis.* Annals of internal medicine, 2015. **163**(1): p. 40-51.

50. *Juxtapid [package insert]. Cambridge, MA: Aegerion Pharmaceuticals, Inc; 2016.*

51. *Kynamro [package insert]. Cambridge, MA: Genzyme Corporation; 2016.*

52. Bloch, K., *The biological synthesis of cholesterol.* Science 150, 1965. p. 19-28.

53. Christians, U., W. Jacobsen, and L.C. Floren, *Metabolism and drug interactions of 3-hydroxy-3-methylglutaryl coenzyme A reductase inhibitors in transplant patients: are the statins mechanistically similar?* Pharmacol Ther, 1998. **80**(1): p. 1-34.

54. Blumenthal, R.S., *Statins: effective antiatherosclerotic therapy.* Am Heart J, 2000. **139**(4): p. 577-83.

55. Helfand, M., S. Carson, and C. Kelley, *Drug class review on HMG-CoA reductase inhibitors (statins).* 2006.

56. Malhotra, H.S. and K.L. Goa, *Atorvastatin.* Drugs, 2001. **61**(12): p. 1835-1881.

57. Thomson, P., *Physician's desk reference 61st ed.* Montvale, NJ, 2007: p. 3171.

58. Sonje, V.M., *et al*., *Atorvastatin calcium*, in *Profiles of Drug Substances, Excipients and Related Methodology*. 2010, Elsevier. p. 1-70.

59. Parke-Davis Div of Pfizer Inc. *LIPITOR- atorvastatin calcium tablet, film coated* 2020, December; [cited 2022 May 25]. Available from: http://labeling.pfizer.com/ShowLabeling.aspx?id=587.

60. Kearney, A.S., *et al*., *The interconversion kinetics, equilibrium, and solubilities of the lactone and hydroxyacid forms of the HMG-CoA reductase inhibitor, CI-981.* Pharm Res, 1993. **10**(10): p. 1461-5.

61. Amly, W. and R. Karaman, *Lipid Lowering Medications-Uses, Side Effects, Pharmacokinetic Properties and Approaches to Improve Bioavailability.* COMMONLY USED DRUGS-USES, SIDE EFFECTS, BIOAVAILABILITY AND APPROACHES TO IMPROVE IT: p. 131.

62. Lea, A.P. and D. McTavish, *Atorvastatin.* Drugs, 1997. **53**(5): p. 828-847.

63. Alshekhlee, A. and B. Katirji, *Clinical perspectives of statin-induced rhabdomyolysis.* The American journal of medicine, 2007. **120**(12): p. e29.

64. Golomb, B.A. and M.A. Evans, *Statin adverse effects.* American Journal of Cardiovascular Drugs, 2008. **8**(6): p. 373-418.

65. Saeed, B., *et al*., *PS1-45: prevalence of statin intolerance in a high risk cohort and management strategies in contemporary cardiology.* Clinical Medicine & Research, 2013. **11**(3): p. 136-136.

66. Banach, M., *et al*., *Statin non-adherence and residual cardiovascular risk: there is need for substantial improvement.* International journal of cardiology, 2016. **225**: p. 184-196.

67. McClure, D.L., *et al*., *Systematic review and meta-analysis of clinically relevant adverse events from HMG CoA reductase inhibitor trials worldwide from 1982 to present.* Pharmacoepidemiology and drug safety, 2007. **16**(2): p. 132-143.

68. Joy, T.R. and R.A. Hegele, *Narrative review: statin-related myopathy.* Ann Intern Med, 2009. **150**(12): p. 858-68.

69. McIver, L.A. and M.S. Siddique, *Atorvastatin*, in *StatPearls*. 2018, StatPearls Publishing

StatPearls Publishing LLC.: Treasure Island (FL).

70. Marcoff, L. and P.D. Thompson, *The role of coenzyme Q10 in statin-associated myopathy: a systematic review.* J Am Coll Cardiol, 2007. **49**(23): p. 2231-7.

71. Yang, B., *et al*., *Atorvastatin pharmacokinetic interactions with other CYP3A4 substrates: erythromycin and ethinyl estradiol.* Pharm Res, 1996. **13**(9): p. S437.

72. Kantola, T., K.T. Kivistö, and P.J. Neuvonen, *Effect of itraconazole on the pharmacokinetics of atorvastatin.* Clinical Pharmacology & Therapeutics, 1998. **64**(1): p. 58-65.

73. Arora, R., M. Liebo, and F. Maldonado, *Statin-induced myopathy: the two faces of Janus.* Journal of cardiovascular pharmacology and therapeutics, 2006. **11**(2): p. 105-112.

74. Toth, P.P., *et al*., *Management of statin intolerance in 2018: still more questions than answers.* American Journal of Cardiovascular Drugs, 2018. **18**(3): p. 157-173.

75. DiMasi, J.A., *The value of improving the productivity of the drug development process.* Pharmacoeconomics, 2002. **20**(3): p. 1-10.

76. Karaman, R., *Using predrugs to optimize drug candidates.* Expert opinion on drug discovery, 2014. **9**(12): p. 1405-1419.

77. Huttunen, K.M., H. Raunio, and J. Rautio, *Prodrugs—from serendipity to rational design.* Pharmacological reviews, 2011. **63**(3): p. 750-771.

78. Abu-Jaish, A., S. Jumaa, and R. Karaman, *Prodrugs Overview*. Nova Science Publishers, Inc. NY, USA, 2014. p. 77-102.

79. Najjar, A. and R. Karaman, *The prodrug approach in the era of drug design*. Expert Opin. Drug Delivery. 2019, **16**: p. 1–5.

80. Karaman, R., *Prodrugs design based on inter- and intramolecular chemical processes.* Chem Biol Drug Des, 2013. **82**(6): p. 643-68.

81. Zawilska, J.B., J. Wojcieszak, and A.B. Olejniczak, *Prodrugs: a challenge for the drug development.* Pharmacol Rep, 2013. **65**(1): p. 1-14.

82. Albert, A., *Chemical aspects of selective toxicity.* Nature, 1958. **182**(4633): p. 421-423.

83. Rautio, J., *et al*., *The expanding role of prodrugs in contemporary drug design and development.* Nature Reviews Drug Discovery, 2018. **17**(8): p. 559-587.

84. Jornada, D.H., *et al*., *The Prodrug Approach: A Successful Tool for Improving Drug Solubility.* Molecules, 2015. **21**(1): p. 42.

85. R Kokil, G. and P. V Rewatkar, *Bioprecursor prodrugs: molecular modification of the active principle.* Mini reviews in medicinal chemistry, 2010. **10**(14): p. 1316-1330.

86. Mueller, C.E., *Prodrug approaches for enhancing the bioavailability of drugs with low solubility.* Chemistry & Biodiversity, 2009. **6**(11): p. 2071-2083.

87. Stella, V.J. and K.W. Nti-Addae, *Prodrug strategies to overcome poor water solubility.* Advanced drug delivery reviews, 2007. **59**(7): p. 677-694.

88. Beaumont, K., *et al*., *Design of ester prodrugs to enhance oral absorption of poorly permeable compounds: challenges to the discovery scientist.* Current drug metabolism, 2003. **4**(6): p. 461-485.

89. Yang, B., *Role of peptide transporter PEPT1 in the intestinal absorption and pharmacokinetics of the amino acid ester prodrug valacyclover* (doctoral dissertation), 2012. Ann Arbor: University of Michigan.

90. Gynther, M., *et al*., *Large neutral amino acid transporter enables brain drug delivery via prodrugs.* Journal of medicinal chemistry, 2008. **51**(4): p. 932-936.

91. Karaman, R., *Design of prodrugs to replace commonly used drugs having bitter sensation.* World Journal of Pharmaceutical Research, 2015. **4**(2): p. 49-58.

92. Chu, W.W., *Prodrug strategies for bypassing the first-pass metabolism of propranolol*. 1987, Dept. of Pharmaceutics, University of Utah.

93. Zhang, J., V. Kale, and M. Chen, *Gene-directed enzyme prodrug therapy.* The AAPS journal, 2015. **17**(1): p. 102-110.

94. Sharma, S.K. and K.D. Bagshawe, *Antibody directed enzyme prodrug therapy (ADEPT): trials and tribulations.* Advanced drug delivery reviews, 2017. **118**: p. 2-7.

95. Huber, B.E., C.A. Richards, and E.A. Austin, *Virus-directed enzyme/prodrug therapy (VDEPT). Selectively engineering drug sensitivity into tumors.* Annals of the New York Academy of Sciences, 1994. **716**: p. 104-14; discussion 140.

96. Merali, Z., S. Ross, and G. Paré, *The pharmacogenetics of carboxylesterases: CES1 and CES2 genetic variants and their clinical effect.* Drug metabolism and drug interactions, 2014. **29**(3): p. 143-151.

97. Jencks, W.P., *Catalysis in chemistry and enzymology*. Mineola, NY, USA: Courier Dover Corporation, 1987.

98. Cooper, G.M., *The central role of enzymes as biological catalysts*, 2nd edn. Sunderland, MA, USA: Sinauer Associates, 2000, p. 145–146.

99. Breijyeh, Z. and R. Karaman, *Enzyme Models—From Catalysis to Prodrugs.* Molecules, 2021. **26**(11): p. 3248.

100. Bruice, T.C. and U.K. Pandit, *Intramolecular Models Depicting the Kinetic Importance of „FIT" in Enzymatic Catalysis.* Proceedings of the National Academy of Sciences of the United States of America, 1960. **46**(4): p. 402.

101. Bruice, T.C. and U.K. Pandit, *The effect of geminal substitution ring size and rotamer distribution on the intramolecular nucleophilic catalysis of the hydrolysis of monophenyl esters of dibasic acids and the solvolysis of the intermediate anhydrides.* Journal of the American Chemical Society, 1960. **82**(22): p. 5858-5865.

102. Bruice, T.C. and F.C. Lightstone, *Ground state and transition state contributions to the rates of intramolecular and enzymatic reactions.* Accounts of chemical research, 1999. **32**(2): p. 127-136.

103. Lightstone, F.C. and T.C. Bruice, *Ground state conformations and entropic and enthalpic factors in the efficiency of intramolecular and enzymatic reactions. 1. Cyclic anhydride formation by substituted glutarates, succinate, and 3, 6-endoxo-Δ4-tetrahydrophthalate monophenyl esters.* Journal of the American Chemical Society, 1996. **118**(11): p. 2595-2605.

104. Milstien, S. and L.A. Cohen, *Stereopopulation control. I. Rate enhancement in the lactonizations of o-hydroxyhydrocinnamic acids.* Journal of the American Chemical Society, 1972. **94**(26): p. 9158-9165.

105. Menger, F.M., *An alternative view of enzyme catalysis.* Pure and applied chemistry, 2005. **77**(11): p. 1873-1886.

106. Brown, R. and N. Van Gulick, *The geminal alkyl effect on the rates of ring closure of bromobutylamines.* The Journal of Organic Chemistry, 1956. **21**(9): p. 1046-1049.

107. Galli, C. and L. Mandolini, *The role of ring strain on the ease of ring closure of bifunctional chain molecules.* European Journal of Organic Chemistry, 2000. **2000**(18): p. 3117-3125.

108. Kirby, A.J. and A. Parkinson, *Most efficient intramolecular general acid catalysis of acetal hydrolysis by the carboxy group.* Journal of the Chemical Society, Chemical Communications, 1994(6): p. 707-708.

109. Brown, C. and A. Kirby, *Efficiency of proton transfer catalysis. Intramolecular general acid catalysis of the hydrolysis of dialkyl acetals of benzaldehyde.* Journal of the Chemical Society, Perkin Transactions 2, 1997(6): p. 1081-1094.

110. Kirby, A. and P. Lancaster, *Structure and efficiency in intramolecular and enzymic catalysis. Catalysis of amide hydrolysis by the carboxy-group of substituted maleamic acids.* Journal of the Chemical Society, Perkin Transactions 2, 1972(9): p. 1206-1214.

111. Karaman, R., B. Fattash, and A. Qtait, *The future of prodrugs–design by quantum mechanics methods.* Expert opinion on drug delivery, 2013. **10**(5): p. 713-729.

112. Karaman, R., *The effective molarity (EM)–a computational approach.* Bioorganic chemistry, 2010. **38**(4): p. 165-172.

113. Karaman, R., *The effective molarity (EM) puzzle in intramolecular ring-closing reactions.* Journal of Molecular Structure: Theochem, 2010. **940**(1-3): p. 70-75.

114. Karaman, R., *Analyzing the efficiency of proton transfer to carbon in Kirby's enzyme model—a computational approach.* Tetrahedron Letters, 2011. **52**(6): p. 699-704.

115. Karaman, R., *The role of proximity orientation in intramolecular proton transfer reactions.* Computational and Theoretical Chemistry, 2011. **966**(1-3): p. 311-321.

116. Karaman, R. and R. Pascal, *A computational analysis of intramolecularity in proton transfer reactions.* Organic & biomolecular chemistry, 2010. **8**(22): p. 5174-5178.

117. Karaman, R., *Reevaluation of Bruice's proximity orientation.* Tetrahedron Letters, 2009. **50**(4): p. 452-456.

118. Karaman, R., *et al*., *Computationally designed atovaquone prodrugs based on Bruice's enzyme model.* Current computer-aided drug design, 2014. **10**(1): p. 15-27.

119. Hashem, F.M., *et al*., *Optimized zein nanospheres for improved oral bioavailability of atorvastatin.* Int J Nanomedicine, 2015. **10**: p. 4059-69.

120. Hashem, F.M., *et al*., *custom fractional factorial designs to develop atorvastatin self-nanoemulsifying and nanosuspension delivery systems–enhancement of oral bioavailability*. Drug design, development and therapy, 2015. **9**: p. 3141.

121. Khan, S., *et al*., *Chlorogenic acid stabilized nanostructured lipid carriers (NLC) of atorvastatin: formulation, design and in vivo evaluation.* Drug development and industrial pharmacy, 2016. **42**(2): p. 209-220.

122. Jain, K., *et al*., *Enhanced oral bioavailability of atorvastatin via oil-in-water nanoemulsion using aqueous titration method*. Journal of Pharmaceutical Sciences and Research, 2013. **5**(1): p. 18.

123. Yin, Y.M., *et al*., *Preparation, characterization and in vitro intestinal absorption of a dry emulsion formulation containing atorvastatin calcium.* Drug Deliv, 2009. **16**(1): p. 30-6.

124. Salama, A.H., M. Basha, and S. El Awdan, *Experimentally designed lyophilized dry emulsion tablets for enhancing the antihyperlipidemic activity of atorvastatin calcium: preparation, in-vitro*

evaluation and in-vivo assessment. European Journal of Pharmaceutical Sciences, 2018. **112**: p. 52-62.

125. Khan, F.N. and M.H. Dehghan, *Enhanced bioavailability of atorvastatin calcium from stabilized gastric resident formulation.* AAPS PharmSciTech, 2011. **12**(4): p. 1077-86.

126. Choi, J.-S. and J.-S. Park, *Surface modification of docetaxel nanocrystals with HER2 antibody to enhance cell growth inhibition in breast cancer cells.* Colloids and Surfaces B: Biointerfaces, 2017. **159**: p. 139-150.

127. Martignoni, M., G.M. Groothuis, and R. de Kanter, *Species differences between mouse, rat, dog, monkey and human CYP-mediated drug metabolism, inhibition and induction.* Expert opinion on drug metabolism & toxicology, 2006. **2**(6): p. 875-894.

128. Mizoi, K., *et al.*, *Synthesis and evaluation of atorvastatin esters as prodrugs metabolically activated by human carboxylesterases.* Bioorg Med Chem Lett, 2016. **26**(3): p. 921-923.

129. Immadi, S., *et al.*, *Improved absorption of atorvastatin prodrug by transdermal administration.* International Journal, 2011. **2229**: p. 7499.

130. Karaman, R., *et al.*, *Computationally designed prodrugs of statins based on Kirby's enzyme model.* Journal of molecular modeling, 2013. **19**(9): p. 3969-3982.

131. Karaman, R., *Antimalarial Atovaquone Prodrugs Based on Enzyme Models-Molecular Orbital Calculations Approach.* Antimalarial Drug Research and Development, Banet, A C. & Brasier, P. Ed, 2013: p. 1-67.

132. Karaman, R., *et al.*, *Design, synthesis and in vitro kinetic study of tranexamic acid prodrugs for the treatment of bleeding conditions.* Journal of computer-aided molecular design, 2013. **27**(7): p. 615-635.

133. Karaman, R., *et al.*, *Prodrugs of acyclovir–a computational approach.* Chemical biology & drug design, 2012. **79**(5): p. 819-834.

134. Karaman, R., K. Dajani, and H. Hallak, *Computer-assisted design for atenolol prodrugs for the use in aqueous formulations.* Journal of molecular modeling, 2012. **18**(4): p. 1523-1540.

135. Karaman, R., *et al.*, *Design, synthesis, and in vitro kinetics study of atenolol prodrugs for the use in aqueous formulations.* The Scientific World Journal, 2014. **2014**.

136. Karaman, R., *et al.*, *Prodrugs of fumarate esters for the treatment of psoriasis and multiple sclerosis—a computational approach.* Journal of molecular modeling, 2013. **19**(1): p. 439-452.

137. Karaman, R., *Prodrugs for masking bitter taste of antibacterial drugs—a computational approach.* Journal of molecular modeling, 2013. **19**(6): p. 2399-2412.

138. Karaman, R., *Prodrugs of aza nucleosides based on proton transfer reaction.* Journal of computer-aided molecular design, 2010. **24**(12): p. 961-970.

139. Karaman, R., *Computational-Aided Design for Dopamine Prodrugs Based on Novel Chemical Approach.* Chemical biology & drug design, 2011. **78**(5): p. 853-863.

140. Karaman, R., *Computationally designed prodrugs for masking the bitter taste of drugs.* J Drug Design, 2012. **1**: p. e106.

141. Karaman, R., *Prodrugs for masking the bitter taste of drugs.* Application of Nanotechnology in Drug Delivery, 2014: p. 399-445.

142. Hejaz, H., R. Karaman, and M. Khamis, *Computer-assisted design for paracetamol masking bitter taste prodrugs.* Journal of molecular modeling, 2012. **18**(1): p. 103-114.

143. Karaman, R., *Computationally designed enzyme models to replace natural enzymes in prodrug approaches.* 2012.

تصنيع، دراسة المواصفات، و دراسة التحلل الذاتي مخبرياً لطلائع جديدة لأتورفاستاتين

إعداد: بثينة أمجد الجعبة

إشراف : البروفيسور رفيق كرمان

ملخص

فرط كولستيرول الدم هو عامل اختطار للإصابة بمرض تصلب الشرايين. يعد دواء أتورفاستاتين دواء اساسياً للوقاية أو العلاج من فرط كولستيرول الدم و أمراض القلب والشرايين التصلبية. أتورفاستاتين يخفض بفاعلية معدل الكولستيرول في الدم عن طريق تثبيط عمل إنزيم 3-hydroxy-3-methylglutaryl-coenzyme A reductase. نتيجة للإستقلاب الهائل ما قبل الوصول للدورة الدموية، يمتلك أتورفاستاتين نسبة ضئيلة من التوافر الحيوي (14%). التعديل المؤقت للبنية الكيميائية للمواد الدوائية عن طريق تصنيع طلائع الأدوية يمكن من إصلاح العيوب المتعلقة بقلة نسبة التوافر الحيوي و عيوب الحركية الدوائية و السلبيات الفيزيوكيميائية الأخرى. هذه الأطروحة تصف البناء الكيميائي لطلائع جديدة لأتورفاستاتين تحمل إمكانية تحسين التوافر الحيوي وتقليل الأعراض الجانبية للدواء. بناء على نموذج إنزيم بروس للتفاعلات الذاتية للجزيئات، تم تصنيع ثلاثة طلائع لأتورفاستاتين عن طريق ربط وصلات (linkers) انهايدرايد ثنائية الكربوكسيل (انهايدرايد الماليك، انهايدرايد السكسنيك، وانهايدرايد الفثاليك) بمجموعات الهيدروكسيل من أتورفاستاتين، من أجل صنع طلائع ذات قدرة تحلل ذاتية. من المتوقع أن تمنح الطلائع الجديدة نسبة توافر حيوي عالية لأنها تخفي المجموعات الكيميائية الحساسة للإستقلاب، وأيضا تمتلك ذائبية عالية في الماء. تم استخدام فحص درجة الانصهار، أطياف الأشعة تحت الحمراء، قياس الطيف الكتلي المقترن بكروماتوغرافيا السائل، والقياس الطيفي بالرنين المغنطيسي النووي للبروتون للتأكد من هوية الطلائع المنتجة. تم دراسة التحلل الذاتي للطلائع الثلاثة مخبرياً في وسائط مختلفة ووجد أن الطلائع تتحلل بمعدلات مختلفة وبعضها لا يتحلل. تبين أن طليعة الأتورفاستاتين المحتوية على وصلة الماليك (ProD1) تحللت كلياً في المحلول الحمضي (0.1N HCl solution)، ودرجة حموضة 3، و بلازما الدم بقيمة عمر النصف 102 ساعة، 161 ساعة، و 198 ساعة، على الترتيب. طليعة الأتورفاستاتين الثانية (ProD2) تحللت فقط في الوسط الحمضي (pH 3) بعمر نصف قدره 216 ساعة. وجد أن درجة حموضة الوسط أثرت على التحلل الذاتي للطلائع حيث كان أكثر سرعة في الوسط ذي درجة الحموضة المنخفضة. إضافة إلى ذلك، التحلل الذاتي اعتمد على خصائص البنية الكيميائية للوصلة المرفقة للطلائع، حيث حصل التحلل في النظام الطلائعي ذي طاقة التوتر الأكبر مع وجود توجه لتقارب مراكز التفاعل بشكل ملائم لحدوث التحلل.